

Florian Preishuber-Pflügl

**Preparation of
Emulsion-templated Porous Polymers via
Ring Opening Metathesis Polymerization**

Master Thesis

Masterarbeit

zur Erlangung des akademischen Grades eines
Diplom-Ingenieurs

der Studienrichtung Technische Chemie
erreicht an der Technischen Universität Graz

Juni 2011

Betreuer: Assoc.Prof. Dipl.-Ing. Dr.techn. Christian Slugovc
Institut für Chemische Technologie von Materialien
Technische Universität Graz

Deutsche Fassung:
Beschluss der Curricula-Kommission für Bachelor-, Master- und Diplomstudien vom 10.11.2008
Genehmigung des Senates am 1.12.2008

EIDESSTATTLICHE ERKLÄRUNG

Ich erkläre an Eides statt, dass ich die vorliegende Arbeit selbstständig verfasst, andere als die angegebenen Quellen/Hilfsmittel nicht benutzt, und die den benutzten Quellen wörtlich und inhaltlich entnommene Stellen als solche kenntlich gemacht habe.

Graz, am

.....

(Unterschrift)

Englische Fassung:

STATUTORY DECLARATION

I declare that I have authored this thesis independently, that I have not used other than the declared sources / resources, and that I have explicitly marked all material which has been quoted either literally or by content from the used sources.

.....

date

.....

(signature)

*gewidmet meinen Eltern,
Maria und Alois Preishuber-Pflügl*

Danksagung

An dieser Stelle möchte ich mich bei all jenen Menschen bedanken, die mich während meines gesamten Studiums, und vor allem während meiner Diplomarbeit so großartig unterstützt und gefördert haben.

Mein besonderer Dank gilt Herrn Prof. Christian Slugovc, für die Bereitstellung des interessanten Arbeitsthemas, für sein stetiges Interesse an den Arbeitsfortschritten, seine Unterstützung, den interessanten Gesprächen, und für die Möglichkeit der Präsentation meiner Arbeit auf einer internationalen Konferenz.

Bei all meinen Arbeitskollegen möchte ich mich für die gute Zusammenarbeit bedanken, für die großartige Arbeitsatmosphäre und für den Spaß in und außerhalb der Uni. Vielen Dank Anita und Sebastijan für die vielen guten Ratschläge, die spannenden Diskussionen und die stetige Hilfsbereitschaft. Weiters gilt mein Dank LiSi und Andi für die tolle gemeinsame Zeit während des Studiums und die guten Freundschaften, die daraus entstanden sind.

Weiters möchte ich mich bei Josefine Hobisch für die GPC-Messungen bedanken, bei Petra Kaschnitz für die NMR Ratschläge, und bei Monika Filzwieser für die Durchführung der Elementaranalysen. Ebenso gilt mein Dank den Kollegen aus Maribor für die Aufnahmen der zahlreichen Bilder am Elektronenmikroskop.

Für die finanzielle Unterstützung gilt mein Dank der Österreichischen Forschungsförderungsgesellschaft (FFG) im Rahmen der Österreichischen Nanoinitiative (Projekt DEVFAB).

Bei meinen Eltern, Alois und Maria, und bei meinen Schwestern, Verena und Julia, bedanke ich mich für die stetige Unterstützung beim Erreichen meiner Ziele, der Ermöglichung meines Studiums, für ihre Liebe und ihr Verständnis, für ihr Interesse an meinem Studium und für ihren stetigen Glauben an mich.

Abstract

Porous polymers have gained significant attention in academic and industrial research in recent years, since they can be tuned in shape, structure and functionality to fulfill the required, specific demands in these materials. PolyHIPEs constitute a special class of this group, featuring a highly ordered macroporosity, which is achieved by emulsion templating. They are prepared by polymerization of the continuous phase of a High Internal Phase Emulsion (HIPE), which also gave this class of porous materials its name. PolyHIPEs were introduced to several fields of research in chemistry, biochemistry and material science addressing various potential applications. Examples comprise such as supporting materials for heterogeneous catalysis, stationary phases for chromatography, growth media for cell culture and tissue engineering for medical, biological and biochemical applications, or usage as a material exhibiting a low dielectric constant for microelectronics.

In the framework of this work, polyHIPEs are prepared via Ring Opening Metathesis Polymerization (ROMP), a rarely employed polymerization technique for polyHIPE preparation. Materials from cyclooctene (COE) and dicyclopentadiene (DCPD) were prepared, with a special focus on the long term stability of these polymers, related to oxidative degradation, as polyDCPD is considered to be prone to oxidation due to its reactive *tertiary* allylic carbons.

Upon variation of the initially considered polymeric surfactant Synperonic L121, that worked perfectly for stabilizing water-in-oil emulsions (W/O) of DCPD, to a small molecule surfactant, namely Span 80, polyHIPEs of pure poly(cyclooctene) were successfully prepared. COE did not form stable (W/O) emulsions using Synperonic L121, thus copolymerization of DCPD and COE did only yield polyHIPE morphology with small amounts of COE. Oxidation stability was investigated with FT-IR measurements and elemental analysis, which has proven poly(cyclooctene) to be less sensitive towards oxygen than polyDCPD.

Kurzfassung

Poröse Polymere haben in den letzten Jahren deutlich an Aufmerksamkeit in der universitären, sowie der industriellen Forschung gewonnen, da diese einfach in Form, Struktur und Funktionalität verändert werden können um so die benötigten, speziellen Anforderungen im jeweiligen Anwendungsgebiet zu erfüllen. PolyHIPEs stellen dabei eine spezielle Klasse dieser Gruppe dar, die sich durch ihre hochstrukturierte Makroporosität, welche durch sogenanntes "emulsion templating" (Formgebung durch Emulsions-Strukturierung) erreicht wird, auszeichnet. Sie werden durch Polymerisation der kontinuierlichen Phase einer High Internal Phase Emulsion (Emulsion mit hohem Anteil an interner Phase) hergestellt, was dieser Klasse poröser Materialien auch den Namen gibt. PolyHIPEs wurden bereits in vielen Bereichen wie der Chemie, der Biochemie und der Materialwissenschaften in sehr unterschiedlichen Anwendungsgebieten getestet. Einige Beispiele wären etwa Trägermaterialien für die heterogene Katalyse, stationäre Phasen für die Chromatographie, Wachstumsmedien für die Zellkultivierung und Gewebezüchtung für medizinische, biologische, oder biochemische Anwendungen, aber auch die Ausnutzung der niedrigen Dielektrizitätskonstante dieser Materialien in der Mikroelektronik.

Im Rahmen dieser Arbeit wurden polyHIPEs mittels Ringöffnender Metathesepolymerisation (ROMP) hergestellt, eine bisher wenig verwendete Polymerisationsmethode für die Herstellung von polyHIPEs. Für die Herstellung der Materialien wurden *cis*-Cycloocten (COE) und Dicyclopentadien (DCPD) verwendet, wobei der Fokus der Arbeit auf der Langzeitstabilität der hergestellten Polymere gegenüber oxidativem Abbau lag, da vor allem Poly(dicyclopentadien) aufgrund der reaktiven *tertiären* allylischen Kohlenstoffe zur Oxidation neigt. Durch das Austauschen des ursprünglich angedachten polymeren Tensids Synperonic L121, welches sehr stabile Emulsionen von Wasser und DCPD bildet, mit Span 80, einem kurzkettigen Tensid, konnten erfolgreich polyHIPEs aus Cycloocten hergestellt werden. Da COE mit Synperonic L121 keine stabilen Wasser-in-Öl (W/O) Emulsionen gibt, ergab nur die Copolymerisation von DCPD mit geringen Anteilen an COE die gewünschte polyHIPE Struktur. Die Oxidationsstabilität der Polymere wurde mittels FT-IR sowie Elementaranalyse untersucht, wodurch die bessere Stabilität von Poly(cycloocten) im Vergleich zu Poly(dicyclopentadien) bestätigt werden konnte.

List of Abbreviations

ADMET	Acyclic Diene Metathesis Polymerization
APS	ammonium persulfate
ATR	attenuated total reflection
CM	Cross Metathesis
COE	Cyclooctene
DCPD	Dicyclopentadiene
DVB	Divinylbenzene
FT-IR	Fourier Transform Infrared Spectroscopy
HIPE	High Internal Phase Emulsion
HLB	Hydrophile-Lipophile Balance
MM	monomer
NMR	Nuclear Magnetic Resonance
O/W emulsion	oil-in-water emulsion
PCy ₃	tricyclohexylphosphine
polyCOE	poly(cyclooctene)
polyDCPD	poly(dicyclopentadiene)
polyHIPE	Polymerized High Internal Phase Emulsion
PPh ₃	triphenylphosphine
RCM	Ring Closing Metathesis
ROM	Ring Opening Metathesis
ROMP	Ring Opening Metathesis Polymerization
SEM	Scanning Electron Microscopy
St	Styrene
STA	Simultaneous Thermal Analysis
TEMED	<i>N,N,N',N'</i> -tetramethylethylenediamine
W/O emulsion	water-in-oil emulsion

CONTENTS

1. INTRODUCTION	10
1.1. <i>Porous Polymers</i>	10
1.2. <i>Overall aim of this work</i>	10
2. GENERAL ASPECTS	11
2.1. <i>Emulsions</i>	11
2.1.1. <i>Emulsion Stability</i>	11
2.1.2. <i>Evolution of an emulsion</i>	13
2.1.3. <i>Surfactant classification</i>	14
2.2. <i>Polymerization mechanism – Ring Opening Metathesis Polymerization (ROMP)</i>	14
2.2.1. <i>Functional group tolerance</i>	16
2.2.2. <i>Living polymerization – copolymers and endgroup functionalization</i>	16
2.2.3. <i>Modification of backbone C=C double bonds</i>	17
2.2.4. <i>Monomer choice</i>	17
2.3. <i>polyHIPEs</i>	19
3. RESULTS AND DISCUSSION	22
3.1. <i>Preparation of porous poly(cyclooctene) monoliths using Synperonic L121 surfactant</i>	23
3.2. <i>Preparation of polyHIPE monoliths using Span 80</i>	33
3.3. <i>Oxidation stability of polyCOE vs polyDCPD</i>	38
3.4. <i>Co-polymerization of DCPD and COE</i>	43
3.5. <i>Preparation of shouldered test bars and mechanical testing of porous polycyclooctene</i>	45
3.6. <i>The surfactant mystery</i>	48
4. CONCLUSION AND OUTLOOK	50
5. EXPERIMENTAL SECTION	51
5.1. <i>Reagents</i>	51

5.2. Instruments	51
5.3. Preparation of porous polymers	52
5.3.1. Porous monoliths	52
5.3.1.1. FPP20	52
5.3.1.2. FPP23-I	53
5.3.1.3. FPP23-II	54
5.3.1.4. FPP28	55
5.3.1.5. FPP29	56
5.3.1.6. FPP30	56
5.3.1.7. FPP32	57
5.3.1.8. FPP55	58
5.3.1.9. FPP84	59
5.3.1.10. FPP104	60
5.3.1.11. FPP108	61
5.3.1.12. FPP114	61
5.3.2. Shouldered test bars	62
5.3.2.1. polyCOE test bars.....	62
5.3.2.2. poly-COE-co-DCPD test bars	62
6. LIST OF FIGURES	63
7. LIST OF TABLES	64
8. REFERENCES	65

1. Introduction

1.1. *Porous Polymers*

The rapid progress in chemistry and its related sciences increases the demand for more and more sophisticated materials and processes. Porous polymer based materials constitute one of these new research fields in material science. Their introduction in the late 1950s led to a steadily growing research and development work towards application in numerous areas. First targets were aimed at ion-exchange resins and adsorbents, but their further development permitted new applications such as supporting materials for heterogeneous catalysis and solid-phase synthesis, polymeric reagents and chromatography media.¹ A common technique for the preparation of porous polymers includes phase separation processes, where the precipitation and former growth of polymer nuclei forms a scaffolding-like porous structure.² Another very elegant method to prepare well defined porous polymer architectures is emulsion templating, which includes the formation of a so called high internal phase emulsion (HIPE), where the continuous phase is subsequently polymerized. These high structurally ordered macroporous materials were termed polyHIPEs (polymerized High Internal Phase Emulsions). The continuous phase can either be aqueous or organic, depending on the type of emulsion. Water in oil (W/O) and oil in water (O/W) emulsions can be distinguished, whereat the solubility of the monomer determines the type.³ Manifold polymerization methodologies were introduced for the preparation of porous polymers, such as polycondensation or living polymerization methods, such as atom transfer radical polymerization (ATRP), nitroxide mediated polymerization and ring opening metathesis polymerization (ROMP).⁴ Moreover, free radical processes, including thermally- and photoinitiated procedures, as well as radiation polymerization, using γ -rays or electron beams were applied to synthesis of porous polymers. In particular radical polymerization and ROMP were applied to polyHIPE preparation, whereas the latter one exhibits a high potential for functionalization of the materials due to the possibility for modification of the C=C double bonds in the polymer back bone, and the living character of ROMP allows grafting of functional monomers at the surface.⁵

1.2. *Overall aim of this work*

This work focuses on the preparation of polyHIPE materials via Ring Opening Metathesis Polymerization, employing *cis*-cyclooctene (COE) and dicyclopentadiene (DCPD) as monomers. The main goal is to achieve polyHIPE morphology via emulsion templated polymerization of cyclooctene. Such a material is considered to be less sensitive to oxidative degradation than polyDCPD, thus providing a higher long term stability of the material. Furthermore, mechanical properties of a COE based polyHIPE material should be investigated. Finally, the scope of copolymerizing COE and DCPD should be evaluated.

2. General Aspects

2.1. *Emulsions*

An emulsion is a heterogeneous mixture of two or more immiscible liquids, where one phase is dispersed in the other one in the form of droplets. The dispersed phase is also referred to as internal phase, and the continuous one as external phase (Fig. 1). Usually one of the two phases is water, or an aqueous solution, and the other one is the oil phase, containing hydrocarbons. Water-in-oil (W/O), and oil-in-water (O/W) emulsions can be differentiated, where the first part in the name indicates the internal phase. If the game is pushed forward, so called double emulsions can be prepared. A water-in-oil emulsion dispersed in water creates a W/O/W emulsion. The other way round forms an O/W/O emulsion.

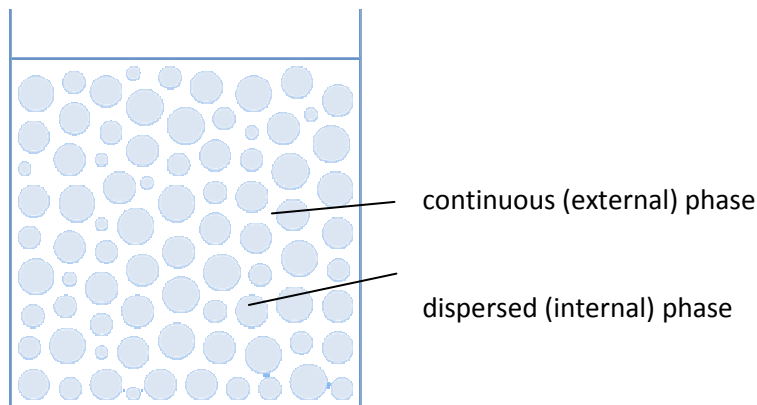


Fig. 1 - Schematic illustration of an emulsion

2.1.1. **Emulsion Stability**

An emulsion is usually prepared by adding one liquid to another, followed by stirring or shaking to disperse large drops to smaller ones in the continuous phase. Every one of us has hopefully at least tried once to prepare a fine salad dressing for a nice dinner, but as the oil was whisked in the vinegar, it separated quickly, and all the effort turned out to be for nothing. More experienced cooks might add a pinch of mustard to succeed, but more on that later.

The reason for the rapid phase separation is explained by thermodynamics in equation 1. The differential Gibb's free energy (dG) rises linear with the increase of surface (dA ; γ represents the interfacial tension).⁶ The surfaces increases upon stirring, as the drops are getting smaller, but increasing their number, resulting in a total increase of the water/oil interface. This is why emulsions are usually prepared by mechanical stirring or treated with ultrasound to provide this required energy. If mixing

2. General Aspects

is interrupted, the drops merge rapidly by releasing free energy, so the process follows the path to lower energy, like everywhere in chemistry.

$$dG = \gamma \cdot dA$$

Equation 1

As mentioned above, experienced chefs add some mustard to the vinegar-oil mixture to obtain a creamy dressing. The reason why we obtain a stable emulsion is the existence of emulsifiers in mustard. These emulsifiers stabilize mixtures of two immiscible liquids, usually by lowering the interfacial tension.⁷ By now, all components to produce stable emulsions are collected: oil, water, and an emulsifier. At this point, we have to distinguish between thermodynamically and kinetically stable emulsions. Thermodynamically stable emulsions, also known as microemulsions, form under certain conditions almost without input of energy.⁸ They can occur as complex, biphasic systems and usually they are transparent due to the small size of the droplets, which ranges from 10-100 nm and below, thus providing the name for this type of emulsions.^{8,9} Kinetically stable emulsions, termed macroemulsions, are thermodynamically unstable dispersions of two immiscible liquids with a droplet diameter of about 0.5-10 μm , usually appearing milky, cloudy, as the droplet size causes scattering of light.¹⁰ High Internal Phase Emulsions (HIPEs) belong to the latter type of emulsions. They are characterized by a high internal volume ratio (Φ), exceeding 74.05 %, which states the densest packing of uniform non-deformable spheres.¹¹

The kinetic stability of macroemulsions depends strongly on the type of emulsifier used. Surfactants (surface active agents) are usually small amphiphilic molecules with a polar head group, and a non-polar, hydrophobic tail. They are classified by their head group, which can either be anionic, cationic, zwitter-ionic or non-ionic. A typical example of an anionic surfactant is given in Fig. 2.

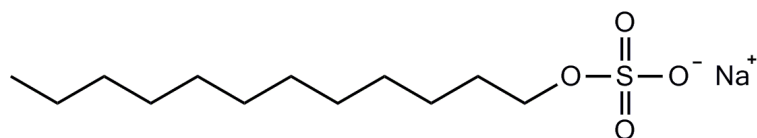


Fig. 2 - Sodium dodecyl sulfate - a typical anionic surfactant

The amphiphilic character of these molecules effects their aggregation at liquid-liquid interfaces to avoid solvophobic interactions. The polar head group tends to solubilize in the aqueous phase, while the hydrophobic tails sticks in the oil phase. This forms a protective layer around the internal phase, thus stabilizing the emulsion droplets. The driving force is the reduction of interfacial tension by the surfactant, resulting in a lower amount of energy required for the formation of small droplets.⁷ Another way to obtain stable emulsions is by sterical stabilization, using solid particles or poly-

mers, as both of them tend to adsorb on surfaces. If the dispersed phase for example does not wet the particle, it will stay out of the drop and be better soluble in the continuous phase. Polymers may as well prefer one of the two phases, depending on the type of repeating units. The solubility properties can be tuned by the use of block-copolymers, which exemplarily contain poly(ethylene glycol) units as the water soluble fragment, and a hydrophobic hydrocarbon fragment.¹²



Fig. 3 - steric stabilization of emulsion droplets - left: solid particles; right: polymers (reprinted from ref 12)

2.1.2. Evolution of an emulsion

A freshly prepared emulsion can undergo several steps towards a total breakup resulting in a complete separation of two phases (Fig. 4).¹² A difference in the densities between the oil and the aqueous phase can cause creaming, where the dispersed droplets migrate to the top of the container. The contrary process is sedimentation, when they sink to the bottom. Droplets that converged due to creaming or flocculation can coagulate, thus forming close aggregates of droplets, while they still keep their individual structure. Coalescence describes the final process, when two drops form a bigger one to reduce interfacial tension. Another emulsion aging process is called Ostwald ripening, where larger droplets grow on expense of smaller ones, due to the higher solubility of the smaller droplets and diffusion of molecules from the internal phase through the continuous phase.¹³

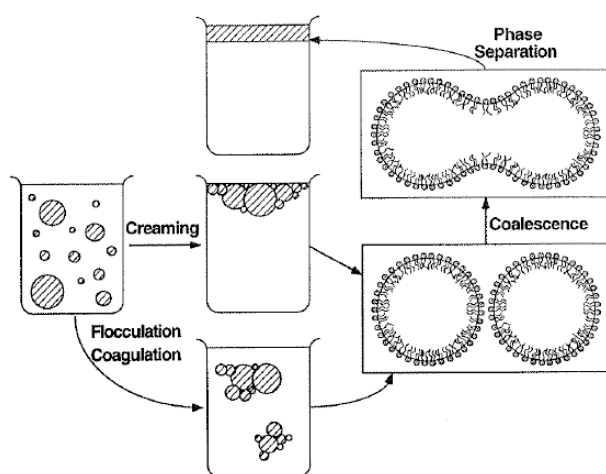


Fig. 4 - schematic illustration of the evolution of a freshly prepared emulsion to the final, complete separation in two phases (reprinted from ref 12)

2.1.3. Surfactant classification

Surfactants do not only stabilize emulsions, but they also determine the type of emulsion (i.e. W/O vs. O/W). Bancroft was the first one who related the emulsion morphology to the different solubilities in one of the two phases, saying an emulsion will be from water-in-oil type if the surfactant is better soluble in the continuous oil phase and vice versa. This empirical prediction is known as Bancroft's rule.¹⁴

To predict the affinity of a surfactant, the HLB concept was introduced in 1955 by Griffin for non-ionic surfactants, whereat HLB stands for Hydrophile-Lipophile Balance. The HLB value is defined by the weight ratio of the hydrophilic part of a surfactant divided by its total molar mass. This ratio is divided by five just to keep the numbers small, ranging from 0-20. HLB values for W/O emulsifiers range from 4-6, and from 8-18 for O/W emulsions, respectively.¹⁵

2.2. Polymerization mechanism - Ring Opening Metathesis Polymerization (ROMP)

Besides several other polymerization methods reported above, ring opening metathesis polymerization is a feasible method for the preparation of porous polymers. The development of well defined, air and water stable ruthenium complexes has paved the way for successful applications of ROMP initiators to various fields of polymer chemistry,¹⁶ including the preparation of emulsion templated porous materials.⁵

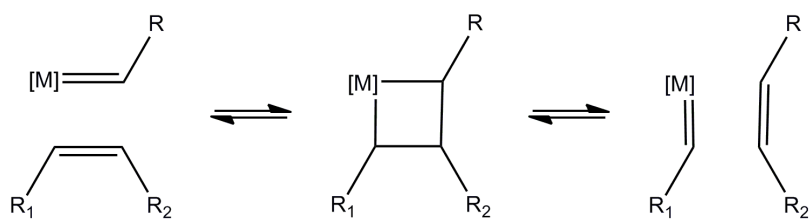


Fig. 5 – reaction mechanism of olefin metathesis (redrawn from reference 16)

Generally spoken, olefin metathesis constitutes a powerful carbon-carbon double bond coupling reaction, catalyzed by transition metals like tungsten or ruthenium. Fig. 5 illustrates the reaction mechanism, which was first proposed by Hérisson and Chauvin in 1971.¹⁷

2. General Aspects

As presented in Fig. 6, metathesis reactions offer plenty of variations, including cross metathesis (CM), ring opening metathesis (ROM), ring closing metathesis (RCM), acyclic diene metathesis polymerization (ADMET), and ring opening metathesis polymerization (ROMP). ADMET and ROMP differ in the polymerization mechanism, as ADMET exhibits a polycondensation-like step growth, releasing an ethylene unit each step, while ROMP represents a classical chain growth polymerization method.

The driving force for ROMP is the ring strain of cyclic olefins. Usually norbornene and its derivatives with a high ring strain of about 27.2 kcal/mol are employed.¹⁸ Low ring strain monomers, like cyclooctene (7.4 kcal/mol),¹⁸ are less frequently used, and may require the use of more active initiators.

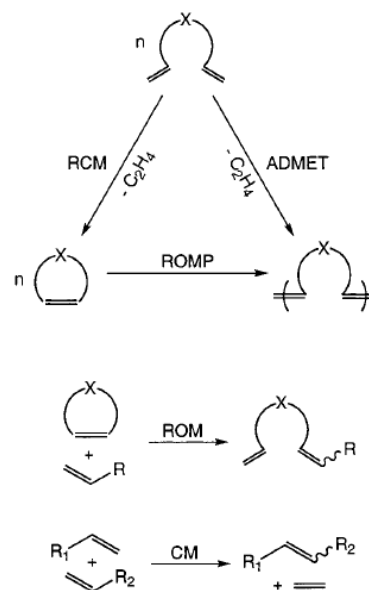


Fig. 6 – olefin metathesis reactions (reprinted from reference 16)

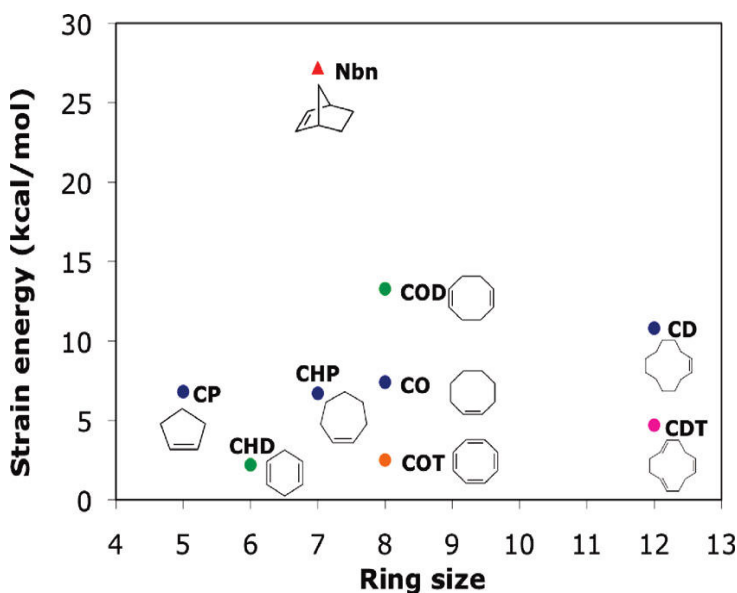


Fig. 7 - plot of ring strain and ring size from cyclic olefins for ROMP (Lerum and Chen, 2011)¹⁹

The attractiveness of ROMP for a multitude of applications is based on the various possibilities for polymer design. The high functional group tolerance of state of the art ruthenium initiators, as well as the living character of the reaction features the creation of highly sophisticated polymers. Besides, ROM polymers exhibit a high degree of unsaturation in their backbone providing a useful site for post-polymerization functionalization. All of these mentioned features will be supported by giving examples to each reaction type.

2.2.1. Functional group tolerance

The high tolerance of ruthenium derived ROMP initiators is to some extent related to their low reactivity towards functional groups. Ruthenium reacts mostly preferred with olefins, followed by acids, alcohol and water, aldehydes, ketones and slowest with esters and amides.¹⁶ This allows the polymerization of numerous functional groups, usually introduced via norbornene derivatives. High tech polymers for organic electronics or liquid crystal polymers were prepared via ROMP, only to point out the versatility of this polymerization method. The demands for special porous materials also led to the introduction of ROMP to this science. Tissue engineering for example often requires deployment of biocompatible and biodegradable material. As a concrete example, the synthesis of biocompatible and -degradable porous monolithic materials by Löber et al. is illustrated in Fig. 8. The polarity of the polymer ensures cell-compatibility allowing ingrowth of cells into the porous media.²⁰

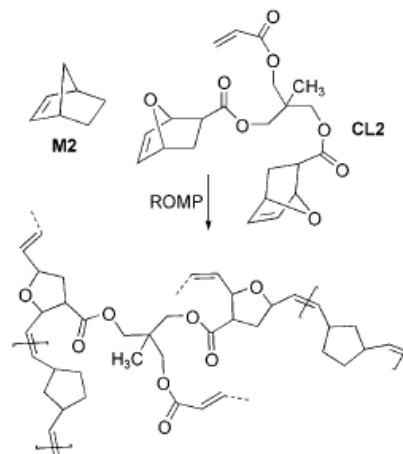


Fig. 8 - reaction scheme for the preparation of biocompatible and -degradable porous monolithic materials from norbornene and functionalized oxanorbornene via ROMP (reprinted from ref 20)

2.2.2. Living polymerization – copolymers and endgroup functionalization

ROMP is considered as a living polymerization, as the metal center remains active at the end of the polymer chain after complete conversion of the monomer.²¹ Hence, block-copolymers are easily available via addition of a second monomer after complete polymerization of a previous one. Deleuze et al. were using this approach for post-functionalization of ROMP-derived polyHIPE material. The polyHIPE itself was prepared via ROMP of tetracyclo [6,2,1^{3,6},0^{2,7}]dodeca-4,9-diene. The internal phase was removed by boiling the monolith in deoxygenated water for 24h, followed by Soxhlet extraction with THF for another 24h. Subsequently, the monolith was immersed in a THF solution of 5-chloromethylbicyclo[2,2,1]hept-2-ene and refluxed for 48h, followed by addition of ethylvinyl ether to deactivate the catalyst. Further purification gave a functionalized ROMP-polyHIPE, as determined by elemental analysis.⁵

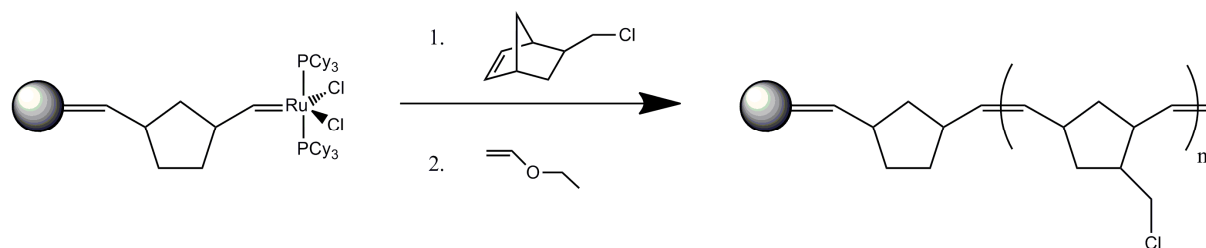


Fig. 9 - surface functionalization of polyHIPE material via living-polymerization (redrawn from ref 5)

2.2.3. Modification of backbone C=C double bonds

The C=C double bonds of ROMP-able monomers are preserved in the polymer and represent another valuable site for post-polymerization functionalization. For example, Thiol-ene “click chemistry” was used to introduce functional groups to ROM polymers. The feasibility of this method has been shown by Wolfberger et al. via photochemically induced crosslinking of poly(norbornene) derived materials using pentaerythritol tetra(3-mercaptopropionate).²² Instead of a thiol-crosslinker, other functional groups, as e.g. catalytic sites, could be introduced to polyHIPE surfaces. Another approach has been demonstrated by Perring and coworkers, employing a more common reaction from organic chemistry for double bond functionalization. MCPBA (*meta*-chloroperoxybenzoic acid) was used for epoxidation of the double bonds to provide a very reactive site for further reactions.²³

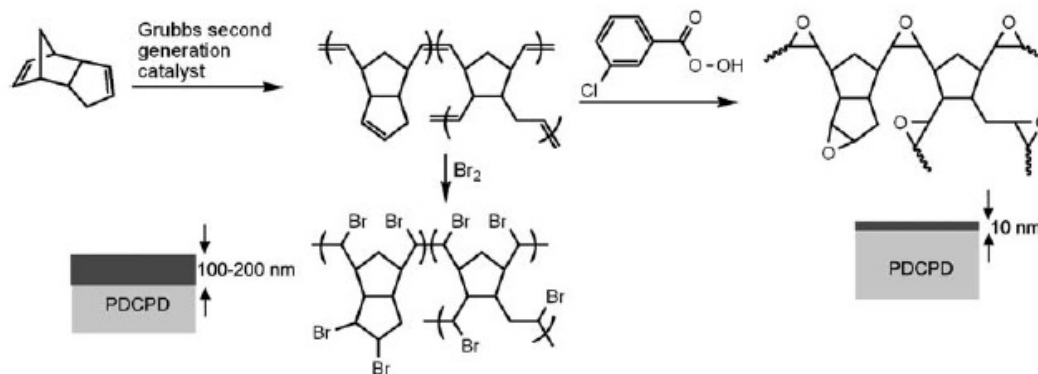


Fig. 10 – epoxidation of polyDCPD using MCPBA (reprinted from ref 23)

2.2.4. Monomer choice

The motivation for using *cis*-cyclooctene as monomer for ROMP has several reasons. First of all poly(cyclooctene) possesses C=C double bonds, which are useful sites for post-functionalization of the material. However, double-bonds are also responsible for the weak long term stability of ROMP-derived materials, as the double bonds are sensitive to oxidative degradation of the polymer. Still,

2. General Aspects

the use of cyclooctene clearly outperforms norbornene-derived polymers in this issue. Poly(norbornenes) possess *tertiary* allylic carbons, while poly(cyclooctene) consists of *secondary* ones. This has an enormous influence on the reactivity of the polymer with oxygen.

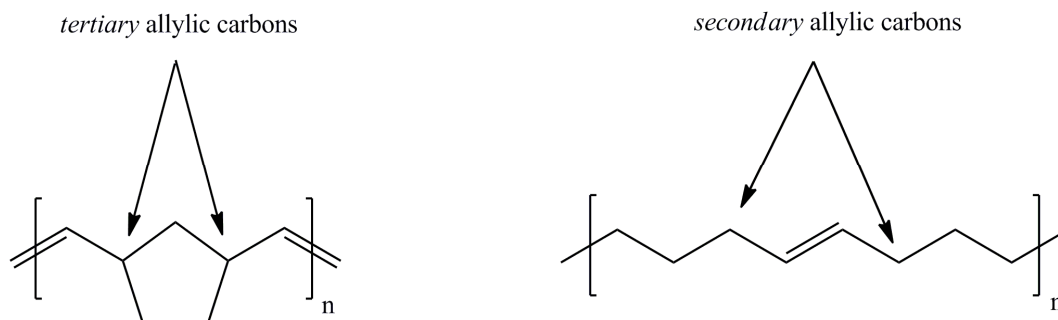


Fig. 11 - location and type of allylic carbons in metathesis polymers – left: poly(norbornene); right: poly(cyclooctene)

The C-H bond strength generally decreases with the degree of substitution, so the proton abstraction is favored in *tertiary* position compared to *secondary* carbons. Vice versa, *tertiary* radicals are most stable, *primary* radicals weakest (Fig. 12). Furthermore, the resonance effect from the neighboring C=C double bond additionally stabilizes the radical.²⁴

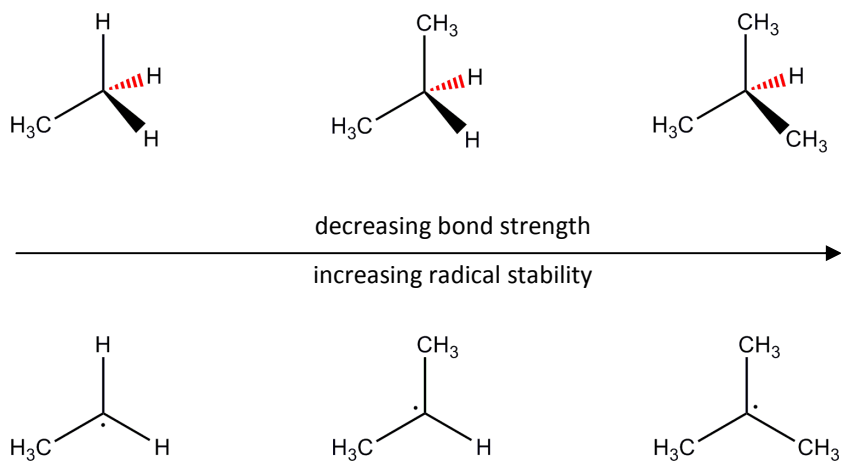


Fig. 12 - radical stability depending on substitution degree

2.3. *polyHIPEs*

PolyHIPEs have undergone an intensive boost in research since their first introduction at Unilever in 1982.²⁵ Their well-defined structure features a highly interconnected porosity, which predetermined their use for chromatographic media. Great interest in this novel class of materials led to their introduction to various fields of academic and industrial research. PolyHIPEs are attractive for their use as low dielectric constant substrates for microelectronic industry, supports for heterogeneous catalysis and synthetic chemistry, membrane support and separations sciences. The wide range of yet employed monomers allowed the production of biocompatible and biodegradable materials that were successfully employed as growth media in tissue engineering and cell culture for medical purposes. Their porous structure has also attracted scientists to use them as templates for the preparation of inorganic porous materials, e.g. for the production of porous electrodes. Hybrid organic-inorganic materials were developed for novel applications such as hydrogen storage, employing metal organic frameworks (MOFs). Recently published reviews provide a further, comprehensive insight to the numerous applications of polyHIPEs mentioned above.^{3,11,26}

The preparation of polyHIPEs is carried out via polymerization of a high internal phase emulsion. As reported in section 2.1.1, the defining feature for a HIPE is its internal phase volume ratio (Φ), of greater than 74.05%, representing the densest packing of uniform, non-deformable spheres. Values of Φ up to 99% were achieved, implying that the size distribution of the droplets is either non-uniform or that they are deformed into polyhedra.^{11,27} The polymerization of the surrounding continuous phase produces a highly ordered polymer skeleton. After removing the internal droplet phase, usually carried out via soxhlet extraction, a well-defined, interconnected macroporous polymer is obtained. A typical polyHIPE structure is shown in Fig. 13. The SEM image shows that the emulsion morphology is preserved in the polymer in the form of large cavities, termed as “voids”. These voids are connected among each other by smaller “windows”, thus producing a totally interconnected porous network. This open cell morphology enables a high permeability of the material, which makes it an ideal candidate for flow-through applications.²⁸

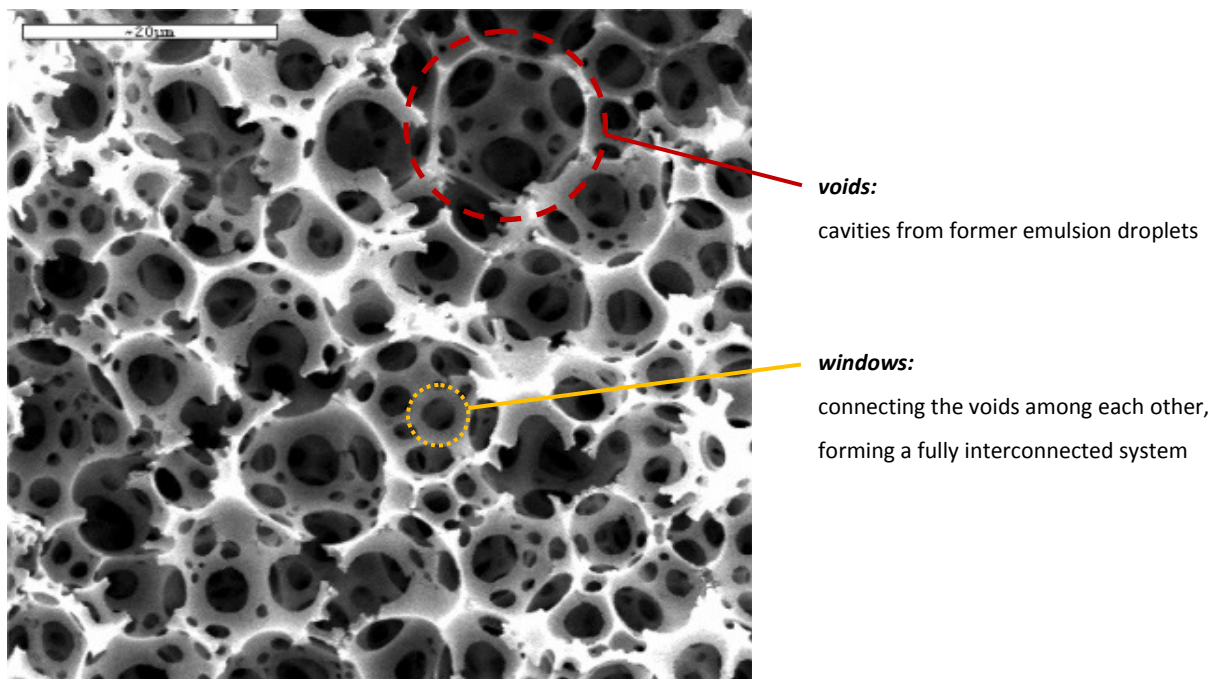


Fig. 13 - SEM image of a typical polyHIPE morphology, marking the typical voids and windows (reproduced from ref 28)

Despite their high porosity, polyHIPEs usually possess a very low surface area due to the large size of the voids. Unmodified styrene-divinylbenzene polyHIPEs (St-DVB polyHIPE), which represent probably the most intensive studied system, exhibit a surface area ranging from 3-20 m² g⁻¹ (determined via BET nitrogen adsorption).²⁹ As polyHIPEs are designed to be used as supports for catalysis or for chromatography, they require much higher surface areas.¹¹ A common way to increase surface area is the incorporation of a non-polymerizable, organic porogen to the HIPE. Sherrington et al. have demonstrated an increase of surface of St-DVB polyHIPEs up to 354 m² g⁻¹ upon incorporation of toluene to the continuous phase of the HIPE.²⁹ The organic solvent undergoes phase separation during polymerization, thus producing small micropores in the polyHIPE walls. Another way to increase surface area, without weakening the material due to the micropores, is hypercrosslinking, which was demonstrated by Pulko et al. for polyHIPE beads from divinylbenzene (DVB) and 4-vinylbenzyl chloride (VBC).³⁰ Lewis acid catalyzed hypercrosslinking of poly(4-vinylbenzyl chloride) was achieved using FeCl₃, increasing the surface area from initial 5.7 m² g⁻¹ to 1100 m² g⁻¹. Additionally, the residual benzyl chloride groups were functionalized with 4-dimethylaminopyridine (DMAP) giving rise to a polyHIPE supported nucleophilic catalyst. Investigations on the catalysis efficiency of this functionalized polyHIPE beads, have shown that the hypercrosslinked material exhibits much better performance than the non-crosslinked one, which outlines the high importance of enhanced surface area for catalytic purposes.

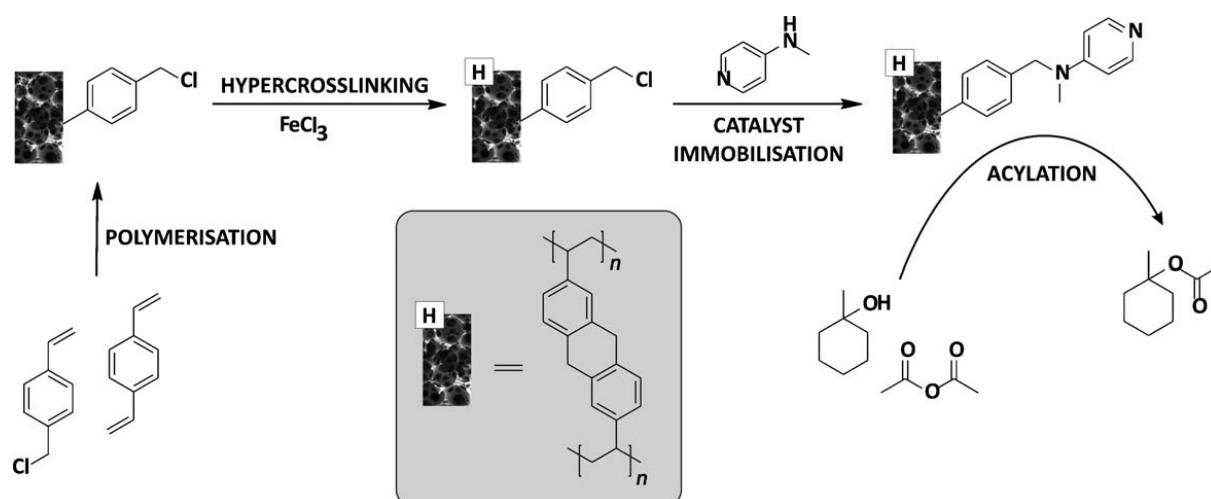


Fig. 14 – schematic illustration of hypercrosslinking and functionalization of DVD-VBC-polyHIPE beads for the nucleophilic acylation of methylcyclohexanol (taken from ref 30)

For the preparation of polyHIPEs, plenty of vinyl- and acrylate-based monomers have been employed, and polymerized via radical polymerization.^{3,11,26} Radical initiators, like potassium persulfate can be thermally triggered by a simple rise of temperature. Redox initiator systems, like ammonium persulfate ($(\text{NH}_4)_2\text{S}_2\text{O}_8$ (APS) and *N,N,N',N'*-tetramethylethylenediamine (TEMED) allow the preparation of polyHIPEs at room temperature, due to their fast initiation.³¹ Photopolymerization of acrylates has been reported using 2,2-dimethoxy-2-phenylacetophenone as photoinitiator.³² The drawback of the latter method may be the polymerization of thick samples, due to the hindered penetration of radiation into the milky emulsion.²⁶ Ring Opening Metathesis Polymerization has also been applied for polyHIPE preparation of norbornene-derived monomers. This polymerization technique is quite new on the field of polyHIPE preparation, compared to radical initiated methods, so that only a few publications are available yet.^{5,33,34} However, the various benefits of ROMP, which were described in detail in section 2.2, may lead to a rapid development in this research area.

3. Results and Discussion

The preparation of polyHIPEs via ring opening metathesis polymerization using ruthenium initiators was first described by Deleuze et al. in 2002.⁵ Grubbs' first generation catalyst (**G1**) was employed for the polymerization of tetracyclo [6,2,1^{3,6},0^{2,7}]dodeca-4,9-diene (BVD) as continuous phase. Due to the high ring strain of the monomer, polymerization proceeded too quickly for a proper handling of the reaction mixture in their first attempts. Upon cooling down a solution of monomer and initiator in dodecane to -15°C, the polymerization was slowed down, and the internal phase was added subsequently. Thus, the polymerization could be controlled more easily and polyHIPEs were successfully prepared via ROMP for the first time. A new approach to synthesize polyHIPEs has recently been described by Kovačič et al.³⁴ A W/O emulsion of water and dicyclopentadiene was stabilized with a surfactant, namely Synperonic L121, (poly(ethylene glycol)-block-poly(propylene glycol)-block-poly(ethylene glycol)), and polymerized with Umicore's **M2** catalyst. The initiator could be homogeneously distributed in the emulsion at room temperature. The curing was then conducted at elevated temperature to increase the activity of the catalyst.

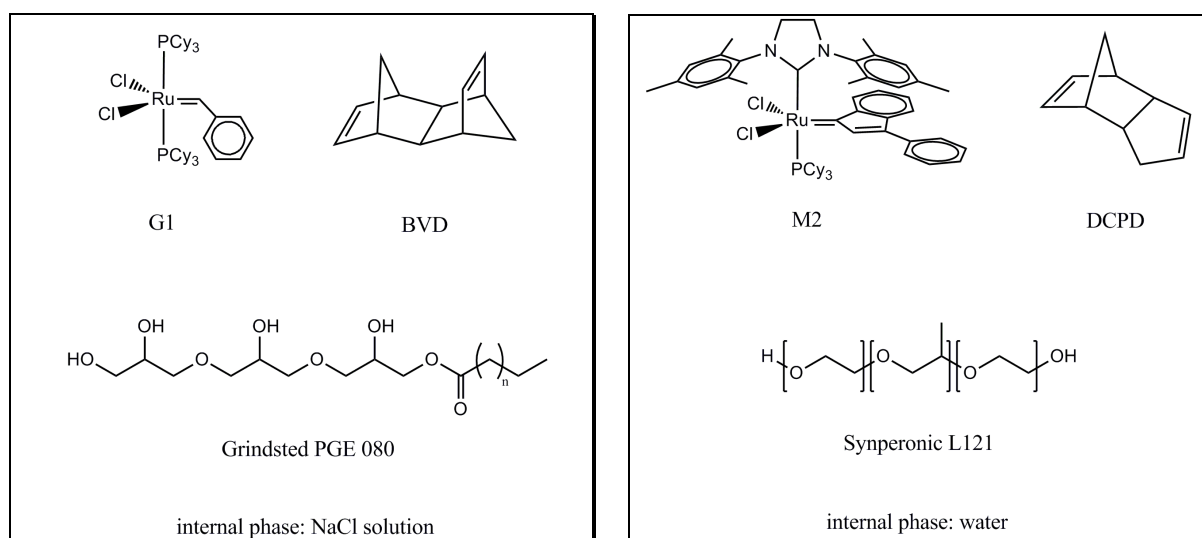


Fig. 15 - polyHIPE preparation via ROMP - left: Deleuze et al. 2002; right: Kovačič et al. 2010

This work focuses on the preparation of polyHIPE materials via ring opening metathesis polymerization of cyclooctene. Established literature procedures were adapted and further developed. In this chapter the route towards the successful synthesis of this novel material is described.

General emulsion preparation procedure

The amount of internal phase was calculated according to equation 2. The ratio was maintained at 0.8 unless indicated otherwise. The amount of surfactant was 15 weight percent referred to the monomer.

$$\Phi = \frac{m_{H_2O}}{m_{H_2O} + m_M + m_s} \quad \text{Equation 2}$$

m_{H_2O} ... mass of internal phase (water) [g]
 m_M ... mass of monomer [g]
 m_s ... mass of solvent for initiator [g]

For the preparation of the emulsion, monomer and surfactant were filled in a 2-necked round bottom flask, equipped with an overhead stirrer. The internal phase (water) was added slowly via a dropping funnel maintaining a rate of one drop every 2-3 seconds. At the beginning of the addition the mixture was stirred gently and after adding some mL of the internal phase the speed was raised to 400 rounds per minute (rpm). After complete addition, the emulsion was stirred at least for another 30 minutes in order to homogenize the droplet size of the internal phase. In the next step, the respective ROMP initiator was dissolved in an organic solvent, usually toluene and added drop-wise to the emulsion at low stirring speed. The mixture was again homogenized at higher speed to distribute the initiator properly. Subsequently, the reaction mixture was transferred to a mold and cured under distinct conditions. The obtained monoliths were extracted with acetone to remove the internal phase and the surfactant, and dried in vacuo in a last step.

3.1. Preparation of porous poly(cyclooctene) monoliths using Synperonic L121 surfactant

First attempts to polymerize cyclooctene HIPes were performed using 0.1 weight percent (w%) M2 in respect to the monomer. Right after the incorporation of the initiator solution, the viscosity of the emulsion increased a little as the polymerization had already started. The sample was cured at 80°C for 4h, resulting in a creamy material with a smooth, firm skin on top. Curing over night did not lead to any further solidification of the material.

Due to the lower ring strain of cyclooctene compared to dicyclopentadiene, the initiator loading was increased to speed up polymerization. A variety of different initiator loadings was tested:

3. Results and Discussion

Table 1 - COE-monolith preparation with increasing initiator loadings

FPP20	COE		Synp.L121	H ₂ O	M2			toluene	M2 : COE
	m [g]	n [mol]	m [g]	V [mL]	m [mg]	w%	n [mol]	V [μL]	
I	1.0168	9.23E-03	0.1479	4.4	1.0	0.1	1.05E-06	200	1 : 8757
II	0.9948	9.03E-03	0.1463	4.4	2.0	0.2	2.11E-06	200	1 : 4284
III	1.0300	9.35E-03	0.1475	4.4	3.0	0.3	3.16E-06	200	1 : 2957
IV	0.9993	9.07E-03	0.1463	4.4	4.0	0.4	4.21E-06	200	1 : 2152
V	1.0184	9.24E-03	0.1416	4.4	5.0	0.5	5.27E-06	200	1 : 1754

The emulsions were prepared with a magnetic stirrer in small glass vials, instead of the usual overhead stirrer on a round bottom flask to simplify the preparation of a variety of initiator loadings with exact amounts. After 1h 20 min the vials were removed from the curing oven. The sample with the lowest loading was still creamy, again with a firm skin on top like in previous attempts. Sample number II with 0.2 w% loading was soft, but not creamy. The samples III-V showed similar characteristics, yet they were a little more rigid. To obtain porous monoliths, the internal phase has to be removed: Vacuum drying did not work out, due to the heavy boiling of the evaporating



Fig. 16 - COE-monolith after extraction with acetone

water. Sample III was directly extracted with acetone, removing both, water and the surfactant in one step. Highly volatile residual acetone could then be easily evaporated. After this procedure, a white, elastic monolith was obtained (Fig. 16). The mechanical stability was poor; the monolith did not return completely to its previous shape upon deformation. To improve this, COE was copolymerized with DCPD, which can act as a crosslinker and thus improve mechanical stability. The monoliths were prepared as follows (Fig. 17):

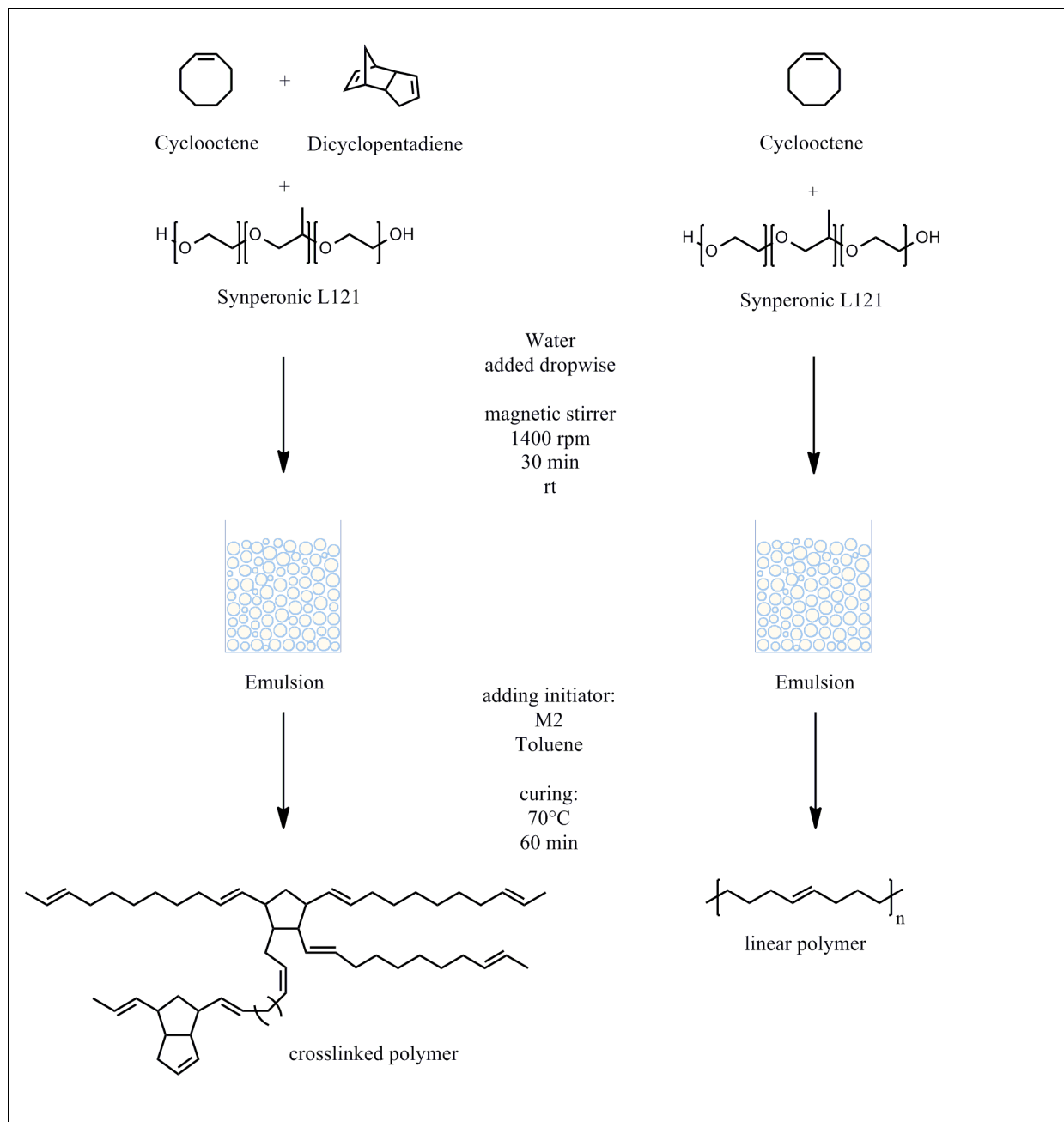


Fig. 17- Scheme for reaction FPP23: preparation of COE-monoliths with DCPD as crosslinker (left) and pure COE (right)

The cured samples were again extracted with acetone and dried in vacuum, as reported above to give solidified monoliths. The incorporation of 5 mol% DCPD to sample FPP23-I already altered the mechanical stability significantly, compared to FPP23-II, a pure COE-monolith. The crosslinked sample was deformed much less than the not crosslinked one, and it recovered its original structure almost completely after deformation.

To study the morphology of the material, scanning electron microscopy was employed. Contrary to all expectations, no polyHIPE structure, but a completely different structure was found. In poly-HIPE materials, so called voids represent the shape of the former internal phase droplets, resulting from the continuous phase around the droplets being polymerized. In our case, no former voids were

visible, and the morphology looked like a 3-dimensional scaffolding (Fig. 18, left). The diameter of the polymer-strings was in the range of 5 to 20 μm , compared to polyHIPE walls that usually have a thickness of about 100-500 nanometers (depending on the internal phase ratio).

Several reasons for this unexpected structure came into consideration. First of all, we assumed that the low melting point of the polymer might have caused a change in the structure. For commercially available poly(cyclooctene), (Vestenamer[®] from Degussa), a melting point of 54°C is reported ($M_w = 90,000 \text{ g/mol}$).³⁵ The emulsions were cured at 80°C, so the temperature was presumably above the melting point of polyCOE. Polymer could have melted right after or during polymerization, followed by subsequent coalescence of molten polymer to form the network. Simultaneous thermo analyses (STA) of the monoliths reveal a melting point of 74.2°C for FPP23-I and 69.2°C for FPP23-II (first melting), which supports this hypothesis.

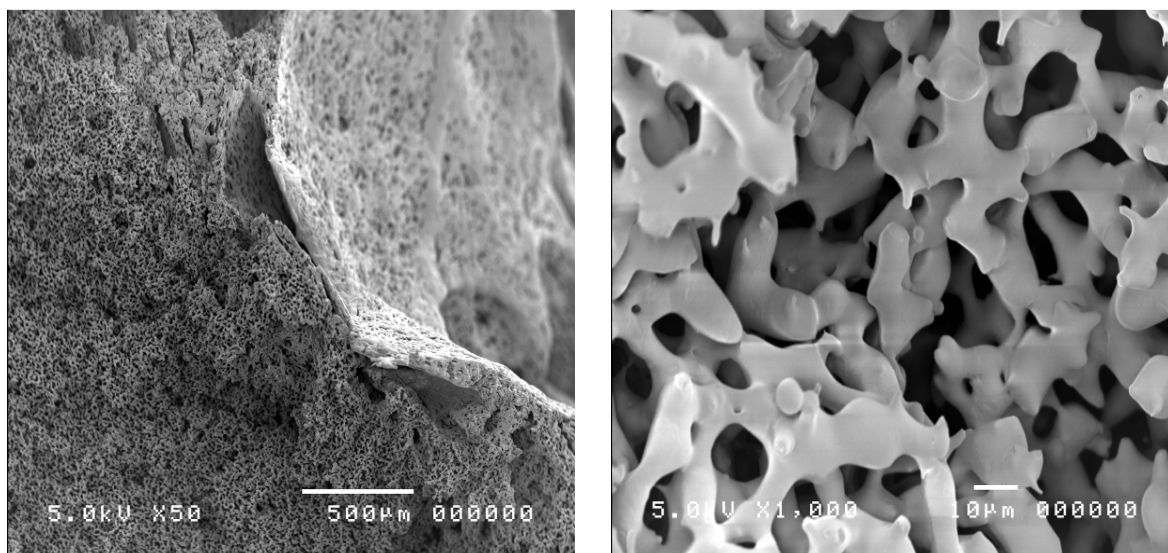


Fig. 18 - SEM images of FPP23-I - left: cross section of the monolith showing the inside and the interface to an air bubble, that was entrapped in the emulsion before polymerization; right: inside of the monolith in high magnification showing the diameter of the polymer-strings

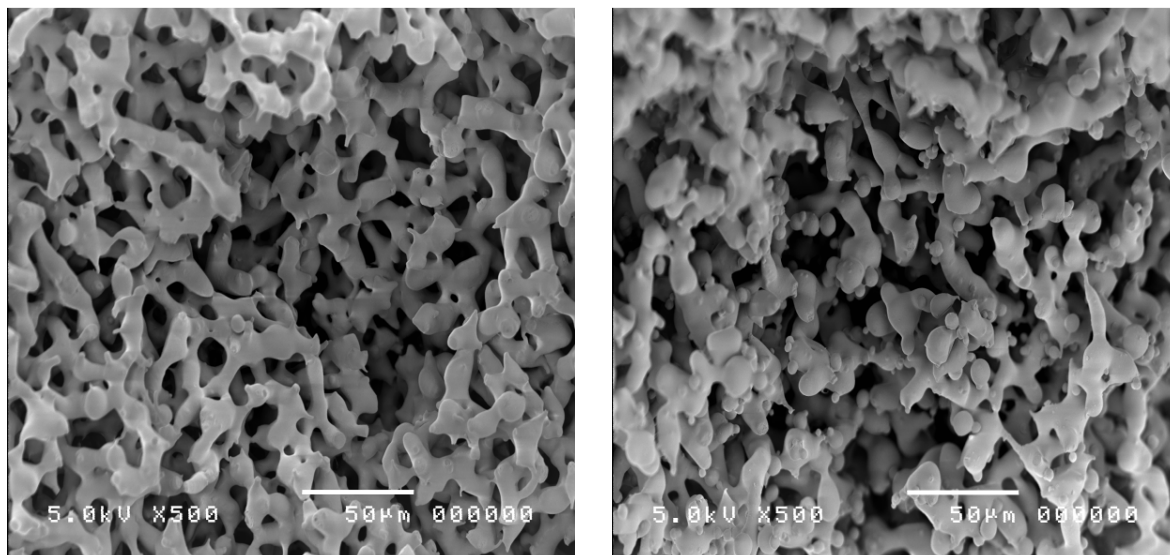


Fig. 19 - comparison of the morphologies of crosslinked cyclooctene (FPP23-I, 5 mol% DCPD; left) and not-crosslinked COE-monolith (FPP23-II; right)

An interesting detail in Fig. 19 permits another assumption for why the polymerization of the emulsion did not lead to a polyHIPE structure. On the right side, the image of the pure COE monolith (FPP23-II) shows small polymer beads, which are attached to the scaffolding-like structure of the monolith. This could indicate that the emulsion has undergone phase inversion, whereupon small micelles and channels of monomer were formed. The lack of beads on the left image of Fig. 19 may be a result of the faster polymerization of the DCPD/COE mixture, due to the high ring strain of DCPD. The rapid polymerization of the oil phase channels would suppress the formation of micelles.

To investigate the previous melting point related hypothesis (cf. above), curing conditions were modified. Emulsions were prepared using an initiator loading of 0.3 w%. Three samples were cured at different temperatures, namely at room temperature (FPP31), at 60°C (FPP32-a) and at 80°C (FPP32-b). For the latter one, 30 min of curing was enough to obtain a soft, elastic monolith. FPP32-was kept in the oven for 1h and 30 min. The sample that was kept at room temperature did not change within 2 days, still exhibiting the reddish color of not activated initiator. The sample was being observed over a longer period. After one month, some polymer particles had formed, but the emulsion had broken. Another attempt at 40°C also failed. The monoliths from reaction FPP32-a/-b were prepared for SEM-analysis by acetone-extraction and vacuum drying.

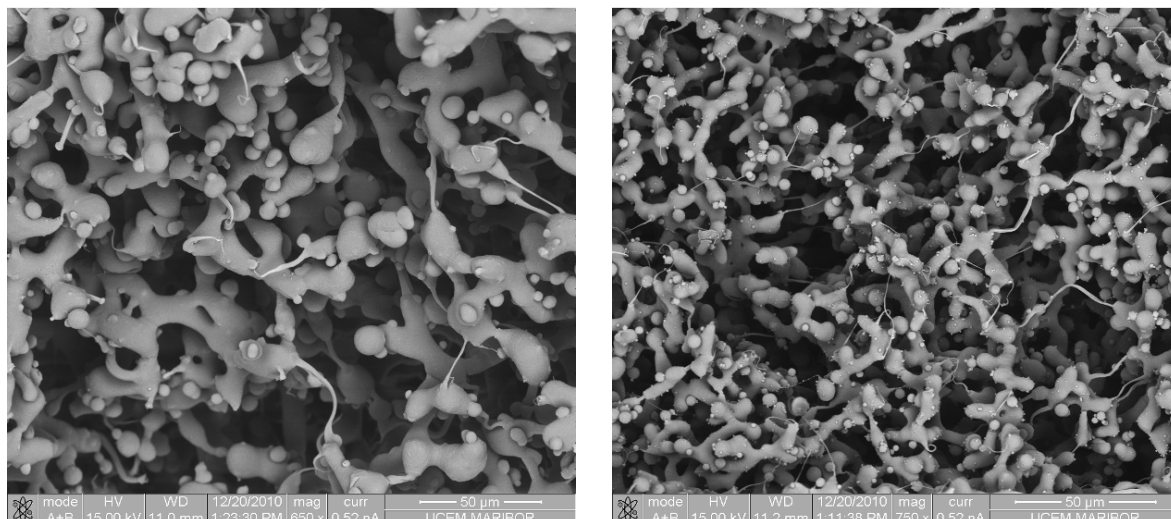


Fig. 20 – comparison of FPP32a (left) and FPP32b (right); curing conditions: a) 60°C, 1h 30 min, b) 80°C, 30 min; initiator loading: 1:3000 (M2:COE)

In spite of lowering the temperature below the melting point of the material, no polyHIPE structure was obtained at 60°C (Fig. 20, left). However, a remarkable structural difference between the samples cured at 60°C and 80°C respectively can be stated. The polymer-strains of the emulsion that was cured at 60°C are much thicker in diameter as the other one cured at higher temperature. This rather indicates instability of the water-in-oil emulsion under these conditions, than that the structure is formed due to melting processes of the polymer. The thicker strains of FPP32a may be a result of coalescence of the oil phase. An explanation can be found in thermodynamics, which generally favors lower energy states: Less strains and an increased diameter of the oil phase channels lead to a reduced surface area, thus a reduction of the surface tension. The reason, why this phenomenon preferentially occurs at lower temperatures is the initiator's thermo responsive mechanism. As there are less active catalyst molecules at lower temperatures, polymerization is slowed down, and monomer droplets can coalesce to form larger drops and channels. At higher temperatures the high number of active initiator molecules causes rapid polymerization and a fast increase of the viscosity. This “freezes” the emulsion and hinders coalescence.

As the stability of the W/O emulsion at high temperatures had turned out to be the crucial factor for the preparation of polyHIPE monoliths, a simple test was carried out. Emulsions with different surfactant concentrations were prepared without any catalyst, and curing conditions were simulated. For a direct comparison, a second mixture containing the surfactant Span 80 was prepared. Span 80 (sorbitan monooleate) is a small molecule surfactant, which has been frequently used for polyHIPE preparations.^{36,37} All samples were prepared with 1 g of cyclooctene, 4.4 mL of water and the amounts of surfactant listed in Table 2.

3. Results and Discussion

Table 2 - emulsion compositions for stability test (FPP28)

sample #	surfactant	HLB	weight %
I	Synperonic L121	0.5	15
II			30
III			20
IV	Span 80	4.3	15
V			30
VI			20

After mixing, the samples were left at room temperature overnight. No phase separation was observed on the next day. To simulate curing conditions, 200 μ L of dichloromethane were incorporated, as this was the usually added amount of initiator solvent, and put in an oven at 60°C. The results confirm the assumption, that Synperonic L121 does not properly stabilize a W/O-emulsion of water and cyclooctene at higher temperatures. After 88 minutes, a high amount of water had accumulated at the bottom of the vials that contained Synperonic L121-stabilized emulsions (Fig. 21). On top of this water layer, residual emulsion remained, which is indicated by the white, milky appearance of the upper phase. The phase separation continued, and after 250 minutes, another layer formed on top of the emulsion, probably due to evaporation and re-condensation of water. The emulsion did not break up completely, but the instability of this mixture is evident. While the mixtures with Synperonic L121 have separated, the emulsions with Span 80 did not visibly change in the same time period, and even after 24h at 80°C, no phase separation was observed.



time = 0 min



time = 88 min



Fig. 21 - emulsion stability test at 80°C; left side, Synperonic L121; right side, Span 80

However, further attempts to prepare polyHIPE with Synperonic L121 were carried out at lower temperatures, as formation of a W/O emulsion at room temperature has been proven by optical microscopy (Fig. 22).

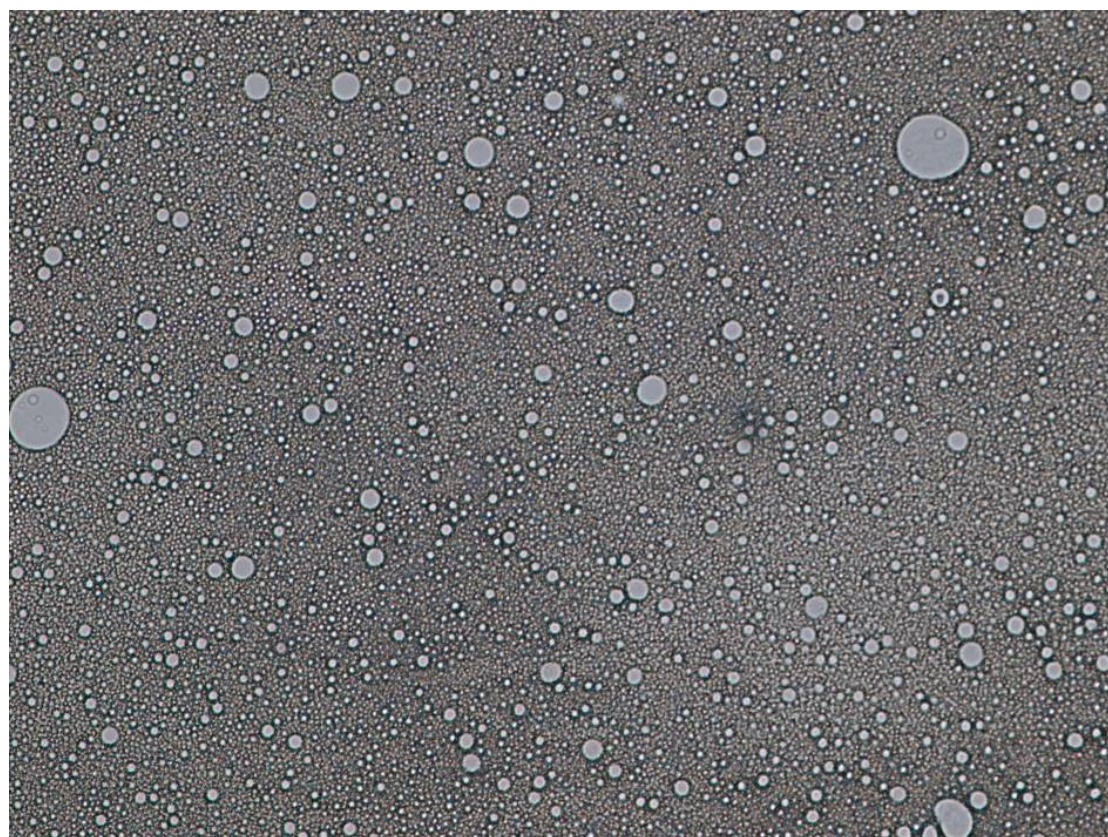


Fig. 22 - optical microscopy images of a W/O emulsion stabilized by Synperonic L121

As reported earlier, the low ring strain of cyclooctene requires the employment of a more active catalyst than M2, which did not show high activity up to 40°C. Therefore, M31 and M51 were chosen due to their fast initiation rates. M31 represents the further development of M2, bearing a pyridine ligand instead of tricyclohexylphosphine. M51 is related to the Grubbs-Hoveyda catalyst featuring a carbene ligand with a chelating ether moiety.

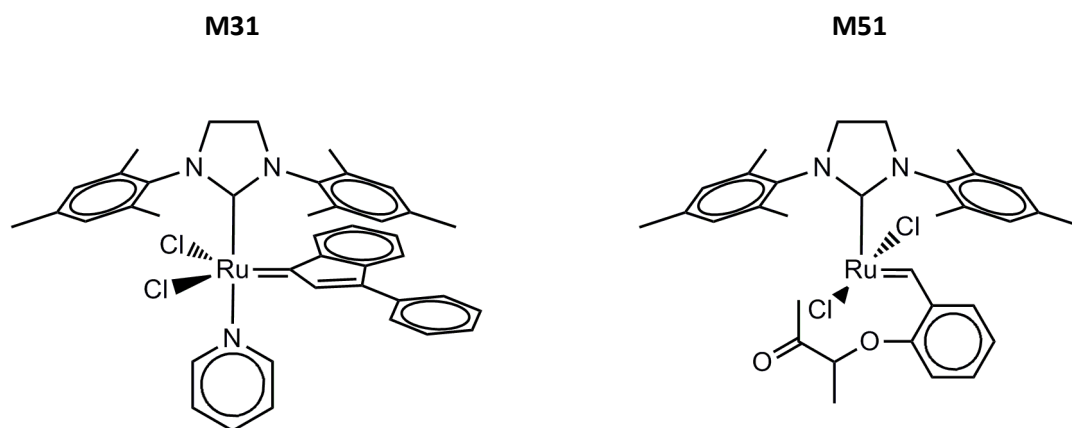


Fig. 23 – M31 and M51; highly active initiators for polyHIPE preparation at low temperatures

A first test was performed with a molar ratio of 9700 : 1 (monomer : initiator) in glass vials using a magnetic stirrer. As soon as the solution of M31 was added, the polymerization proceeded extremely fast and the stirring bar got stuck in the mixture. This led to an inhomogeneous distribution of the initiator in the emulsion, so that most of it remained uncured. M51 showed similar performance, so both of the catalysts were “too fast” for polyHIPE preparation under this conditions. As there was no obvious difference in polymerization speed, only M31 was chosen for further experiments to modify the polymerization conditions. A summary of the reaction conditions is given in Table 3:

Table 3 – summary of monolith preparation using M31

Reaction #	Initiator loading	Conditions	T / °C	comment
FPP18	9700 : 1		20°C	Immediate polymerization, too fast
FPP37	10000 : 1	The emulsion was cooled down to 0°C. Immediate polymerization upon addition of M31; homogeneous distribution of initiator impossible.	0°C	
FPP38	25000 : 1	Fast polymerization; solid and creamy parts. Mixture transferred to mold; extracted with acetone. Pores with diameters of mm-size.	0°C -> 20°C	
FPP21 - I	50975 : 1		20°C / 60°C	firm skin on top, inside creamy; white liquid upon curing in oven

3. Results and Discussion

Inhibition of initiator with pyridine			
FPP19	9700 : 1	M31 : Py 1 : 229 Activation with HCl	20°C
		The pyridine inhibited the polymerization, homogeneous distribution of the catalyst successful; addition of a few drops of HCl started the polymerization, but did not lead to a solid monolith after curing at 80°C	
FPP39	25000 : 1	M31 : Py 1 : 101	0°C / 80°C
		Initiator was added to cooled emulsion (0°C); slow polymerization. Mixture was transferred to a mould and cured at 80°C. No solidification achieved.	
FPP41	25000 : 1	M31 : Py 1 : 50	0°C -> 20°C
		Like FPP40, creamy mixture, but no solid material obtained.	
FPP40	25000 : 1	M31 : Py 1 : 10	0°C -> 20°C
		Immediate polymerization upon addition of initiator; creamy material obtained, no proper solidification.	
FPP21 - II	50975 : 1	M31 : Py 1 : 286	20°C / 60°C
		FPP21-I gave a creamy mixture with a firm skin on top; FPP21-II did not polymerize at all due to pyridine inhibition; rising the curing temperature from 20°C to 60°C over night did not give any solid material	

The tests with M31 have shown that the initiation of the catalyst is proceeding too fast. A homogeneous distribution of the initiator in the emulsion was not possible, so that no processable mixtures were obtained. With high catalyst loadings, local immediate polymerization of the emulsion causes the polymer to wrap around the stirrer, so that it cannot be transferred to a mold. Cooling down the emulsion in an ice bath to 0°C did not slow down the polymerization speed appreciably. Even after lowering the loading to 25000 : 1 polymerization proceeded fast, though a highly viscous mixture could be transferred to a mold and solidified. Soxhlet extraction led to a solid material with very large pores in millimeter size. This may be a result of extracted monomers and oligomers, indicating that the low initiator loading is not sufficient for a complete conversion of the monomer. Inhibition of the catalyst with pyridine did also not lead to satisfying results. Too much pyridine on high initiator loadings completely inhibits solidification. A lower pyridine/M31 ratio, using less M31 gives processable emulsions; however, no noticeable polymerization was observed.

3.2. Preparation of polyHIPE monoliths using Span 80

As all attempts to prepare polyHIPEs from poly(cyclooctene) using Synperonic L121 failed, Span 80 was employed as surfactant. A previous test has proven excellent emulsion stability, even at a high temperature of 80°C (Fig. 21). M2 was again used for polymerization, as the emulsions were very well processable, even after the incorporation of the initiator.

First of all, various loadings of M2 were tested as before for Synperonic L121-emulsions. Samples a)-e) were cured for 1h at 60°C, f) was kept at room temperature.

Table 4 - overview for tested initiator loadings for Span 80 stabilized emulsions

FPP29	COE		Span 80	H ₂ O	M2		DCM	M2:COE	
	m [g]	n [mol]			m [mg]	w%			n [mol]
a	1.0102	9.17E-03	0.1531	4.4	1.0	0.1	1.05E-06	200	8700
b	1.0050	9.12E-03	0.1640	4.4	2.0	0.2	2.11E-06	200	4328
c	1.0047	9.12E-03	0.1561	4.4	3.0	0.3	3.16E-06	200	2884
d	1.0087	9.15E-03	0.1501	4.4	4.0	0.4	4.21E-06	200	2172
e	1.0071	9.14E-03	0.1469	4.4	5.0	0.5	5.27E-06	200	1735
f	0.9970	9.05E-03	0.16320	4.4	2.0	0.2	2.11E-06	200	4293

Dichloromethane (DCM) was used instead of toluene to dissolve the catalyst. The low boiling point (39.7°C) caused the formation of large bubbles in the material due to evaporation of the solvent. DCM was therefore not further used for samples cured at high temperature.

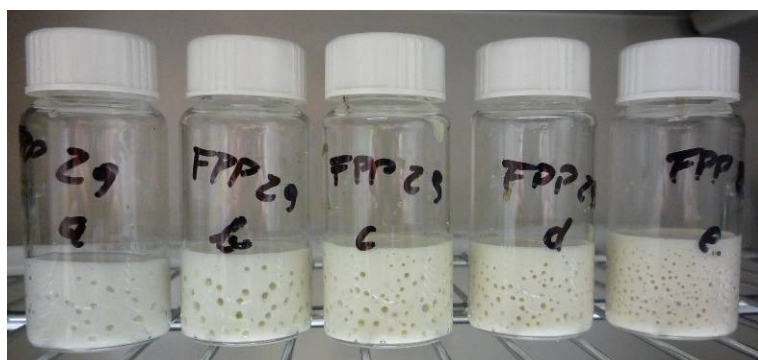


Fig. 24 - Evaporating dichloromethane generates large bubbles

Directly after the samples had been removed from the oven, they were highly viscous and no solid material was obtained. The curing temperature was too close to the melting point of the material. After cooling down to room temperature, c), e) and f) solidified to a very brittle material. Sample a) was still creamy; b) was very soft, providing evidence that the amount of initiator was not high enough. After curing sample f) at room temperature for 1 day, a cloggy mixture was obtained. Re-

3. Results and Discussion

markably, the emulsion had not separated, yet the temperature was too low for a proper polymerization. To improve mechanical stability, DCPD was added as a crosslinker. As a reference also pure DCPD emulsions with Span 80 were prepared. Toluene was used to dissolve the initiator.

Table 5 – amounts for the preparation of pure COE-, pure DCPD-, and co-polymer-monoliths

FPP30	COE		DCPD		Span 80	H ₂ O	M2		M2 : MM
	m [g]	n [mol]	m [g]	n [mol]	m [g]	V [mL]	m [mg]	n [mol]	
a	1.0134	9.20E-03	-	-	0.2028	4.4	3.0	3.16E-06	2909
b	1.0003	9.08E-03	-	-	0.2201	4.4	5.0	5.27E-06	1723
c	0.9491	8.61E-03	0.0583	4.41E-04	0.1965	4.4	3.0	3.16E-06	2864
d	0.9570	8.68E-03	0.1142	8.64E-04	0.1925	4.4	5.0	5.27E-06	1812
e	-	-	0.9995	7.56E-03	0.1866	4.4	1.0	1.05E-06	7176
f	-	-	1.0000	7.56E-03	0.2056	4.4	2.0	2.11E-06	3590

The samples were cured for 1h 30 min at 60°C. Already after 15 min, the DCPD containing emulsions did not flow any more upon tilting the molds, while sample a) and b) were still viscous and remained so even after 1h 30 min. Cooled down to room temperature, all samples were solid, but COE-containing polymers were again very cloggy. The addition of DCPD did not alter the mechanical stability noticeably. The pure DCPD monoliths gave a solid material and were further cured for additional 48 h at 60°C in order to evaporate the internal phase. Yellow monoliths were obtained in one solid piece exhibiting high rigidity. The yellow color of the monoliths results from the rapid oxidation of polyDCPD at elevated temperatures.

The brittleness was a significant drawback of the monoliths, prepared with Span 80. However, a higher initiator loading of 1000 : 1 (COE : M2) was tested (reaction FPP55). Interestingly, after the addition of M2, the viscosity of the emulsion did not rise as quickly as with Synperonic L121. This suggests that the chemistry of the surfactant itself has an important influence on the polymerization behavior of the catalyst. The emulsion was cured at 82°C for 33 minutes, resulting in a grey, highly viscous mass, which solidified after cooling to room temperature. Instead of Soxhlet extraction, acetone was directly pumped through the monolith using pressurized air. The extract was slightly yellow, indicating that the surfactant was washed out of the monolith. Despite the high initiator loading, the material was still very brittle. Another emulsion with 75% internal phase containing COE with 5 mol% DCPD was prepared, to see whether the porosity of the material would influence the mechanical properties. Scanning electron microscopy was used to characterize the morphology the prepared monoliths.

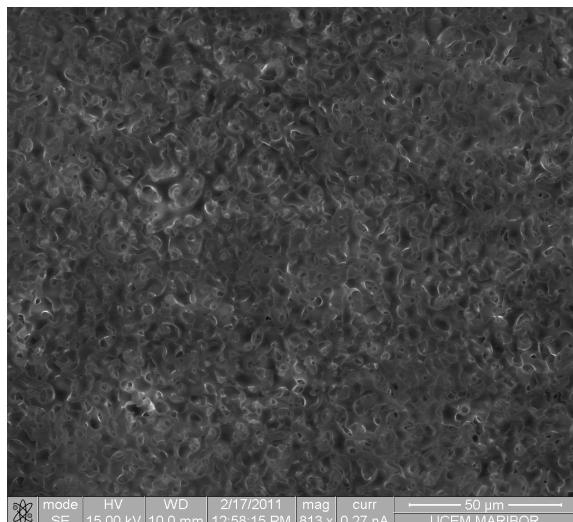


Fig. 25 - SEM image from polyDCPD-monolith prepared with Span 80 (FPP30e)

The promising DCPD monolith prepared with Span 80 did not exhibit polyHIPE morphology. Again, a porous material with a 3-D network structure was obtained (Fig. 25). The analysis of the material obtained from the Span 80-stabilized emulsion from pure cyclooctene finally shows polyHIPE morphology (Fig. 26). This is very interesting, as the emulsion was cured at 80°C, i.e. above the melting point of the polymer – resulting in the fact, that the samples were always still very viscous directly after they had been removed from the oven. However, the polyHIPE structure was preserved and solidified upon cooling. This observation now clearly disproves the previous assumption that the melting of a former polyHIPE lead to a non-HIPE morphology like in the porous poly(cyclooctene) prepared with Synperonic L121 (see page 26).

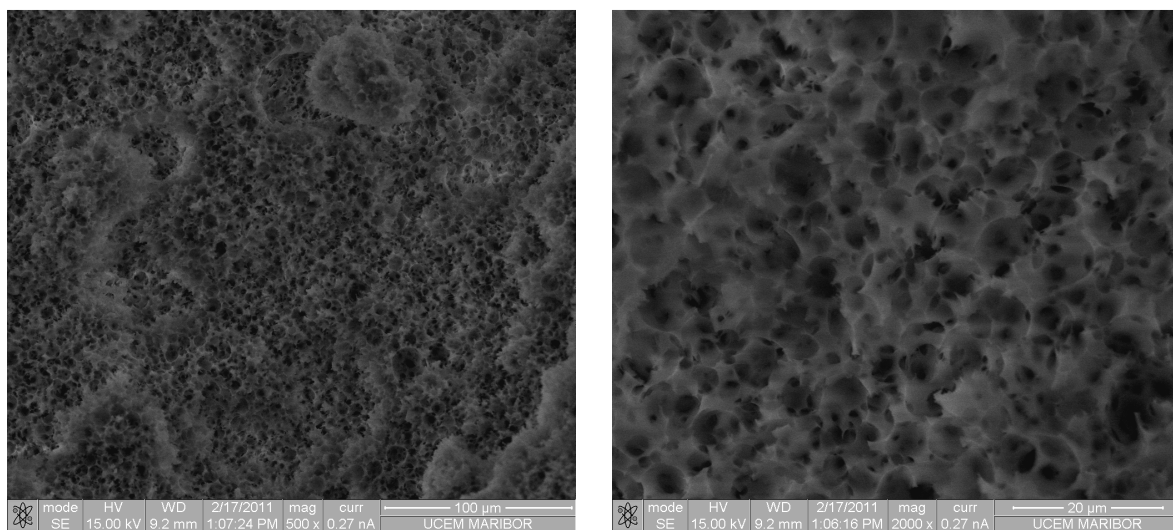


Fig. 26 - morphology of pure polyCOE monolith (80% porosity); SEM in low vacuum mode (FPP55)

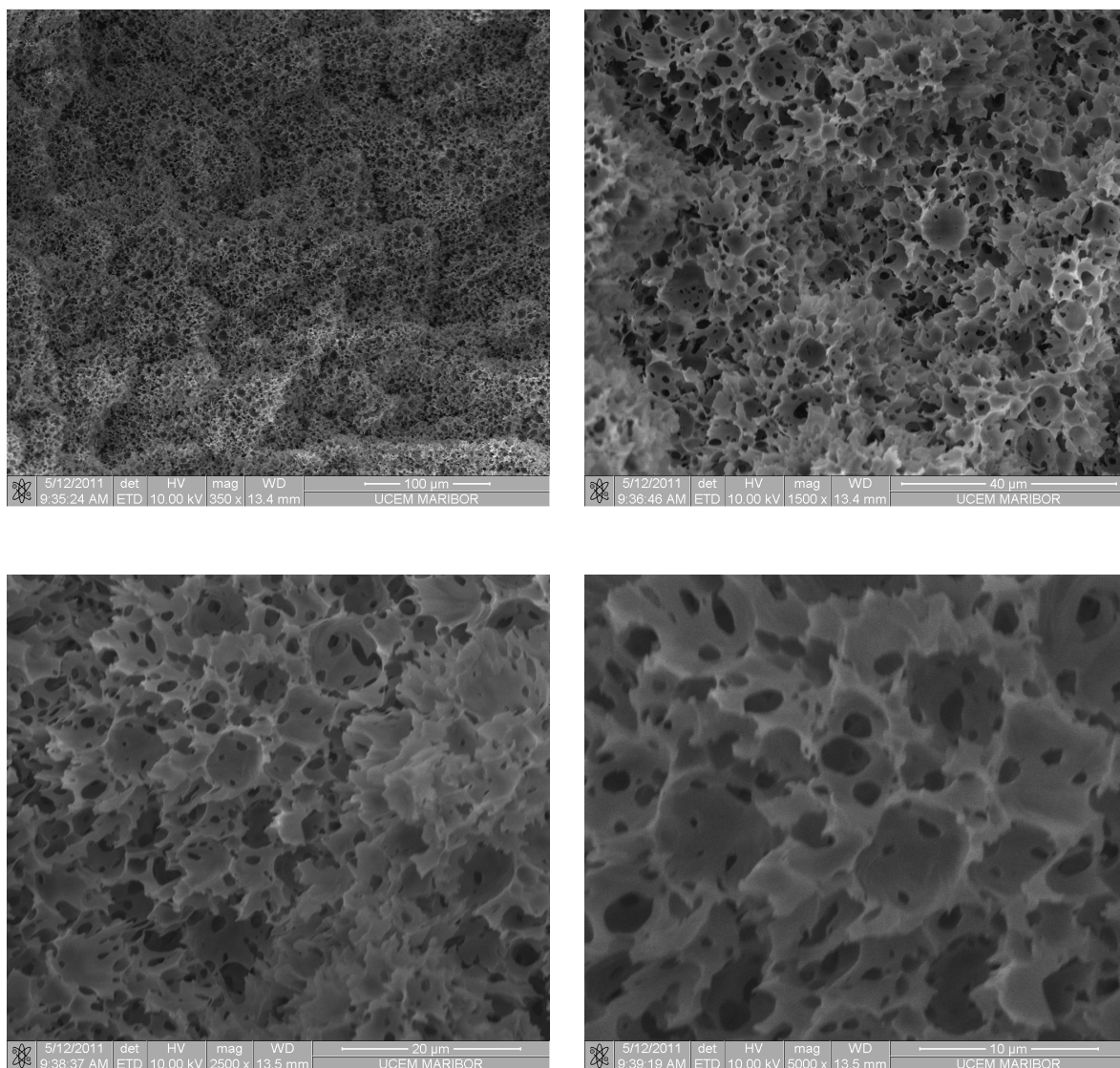


Fig. 27 - COE-co-DCPD-polyHIPE (5 mol% DCPD. 75% porosity; FPP 84)

Although polyHIPEs could be prepared from a W/O emulsion with Span 80 at 80°C, the thermal properties of poly(cyclooctene) suggest a fabrication procedure at lower temperatures. An initiator showing a moderate activity that lies between the high active M31 and the more latent M2 was required. Broggi et al. recently published an article about the influence of the phosphine substituents on the catalytic activity of M2 related initiators.³⁸ M20, which is commercially available, was tested for poly-HIPE preparation at room temperature. Instead of PCy₃ it bears a triphenylphosphine (PPh₃) ligand (Fig. 28). PPh₃ is more labile than PCy₃ due to the electron withdrawing character of the phenyl groups, resulting in a faster initiation behavior. A first attempt with a loading of

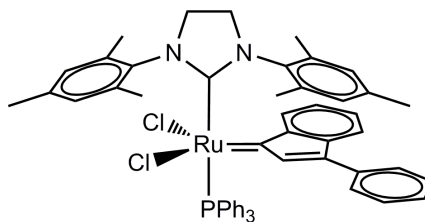


Fig. 28 - M20: ROMP initiator bearing a PPh₃ ligand

3. Results and Discussion

2036 : 1 was carried out (FPP104). After incorporation of the initiator, the emulsion was still very well processable and the mixture could be easily transferred to the glass mould. After five minutes the emulsion's color turned from reddish to white, indicating complete activation of the initiator. 15 minutes later, the mixture had solidified to a white, solid monolith. The material was again very brittle, exhibiting small fissures in the middle, probably due to shrinking of the material. SEM imaging proved polyHIPE morphology.

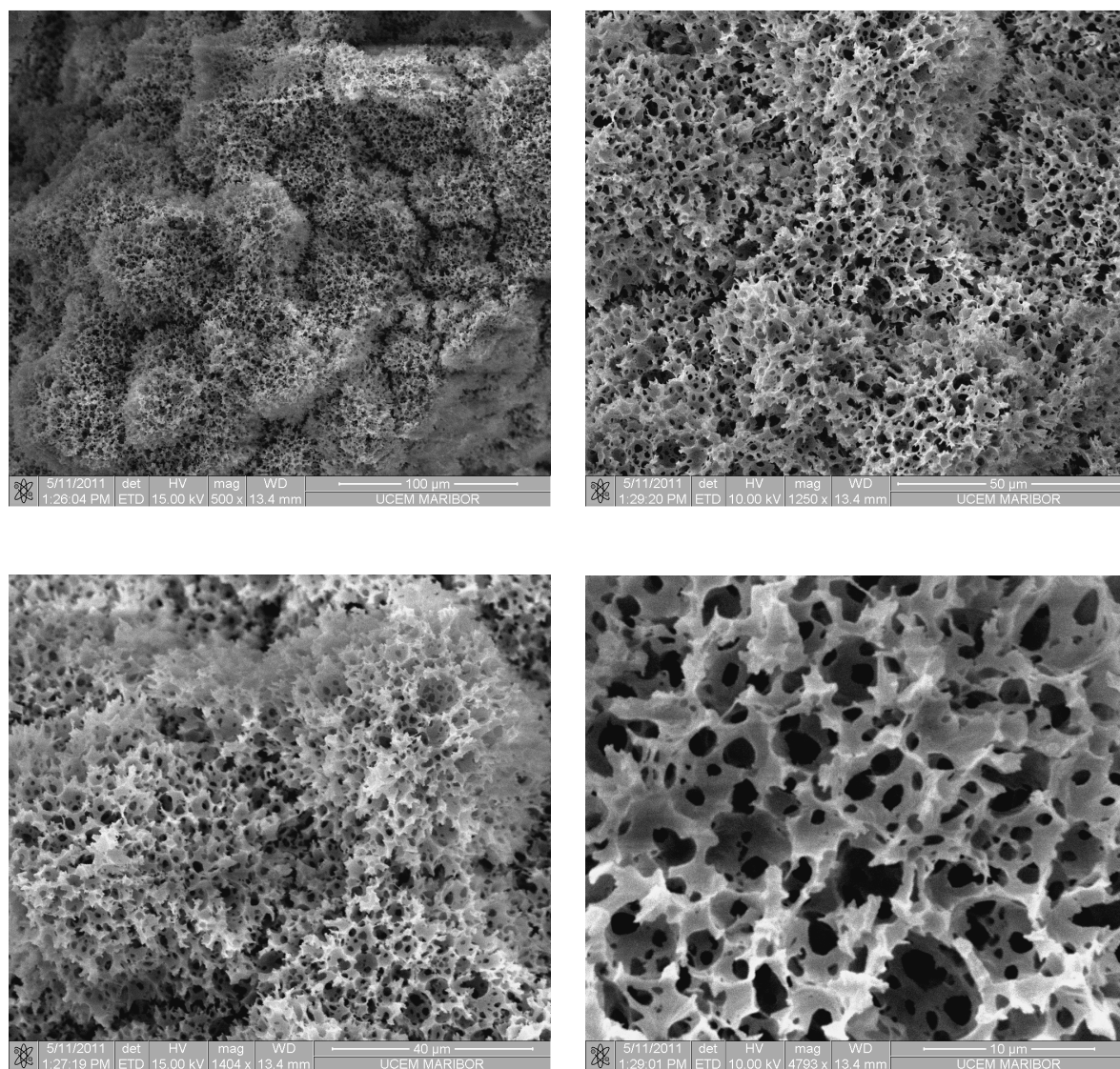


Fig. 29 - COE-polyHIPE prepared at room temperature exhibiting high open-cell morphology (FPP104)

Another important reason for a preparation of polyHIPEs from cyclooctene at lower temperatures is the possibility to post-crosslink the material using thiol-ene chemistry. The crosslinking process is usually triggered upon heating to generate thiol radicals that will then react with the C=C double bonds. In case the ROMP initiator is as well activated by heat, the two reactions will occur simulta-

neously. As a result, the olefinic monomers would also react with thiol radicals and lose the double bond, thus producing a ROMP-inactive molecule.

This approach was originally intended to improve mechanical stability of polyHIPEs, but was not further investigated within this thesis.

3.3. Oxidation stability of polyCOE vs polyDCPD

As described above, polyDCPD is very sensitive to oxidative degradation due to its *tertiary* allylic carbons, which was a cogent reason for the preparation of polyHIPEs from cyclooctene. A significant slower aging of COE-polyHIPEs was expected due to the present *secondary* allylic carbons, which are less reactive regarding hydrogen abstraction and radical formation.³⁹ Additionally, DCPD possesses almost twice as many double bonds as cyclooctene (DCPD: two C=C double bonds per ten carbon atoms; COE: one double bond per eight carbon atoms), so besides the higher sensitivity also the number of potential reaction sites is higher.

Oxidation of the material was followed over time by FT-IR measurements. Porous COE-monoliths prepared from Synperonic L121 stabilized emulsions as well as polyHIPE-monoliths from COE and DCPD were tested. Therefore, fresh samples were prepared, extracted with acetone overnight and dried in vacuo. The samples were exposed to air and sunlight to accelerate the aging process. Peak assignment was done by comparison with tabulated values from literature.⁴⁰

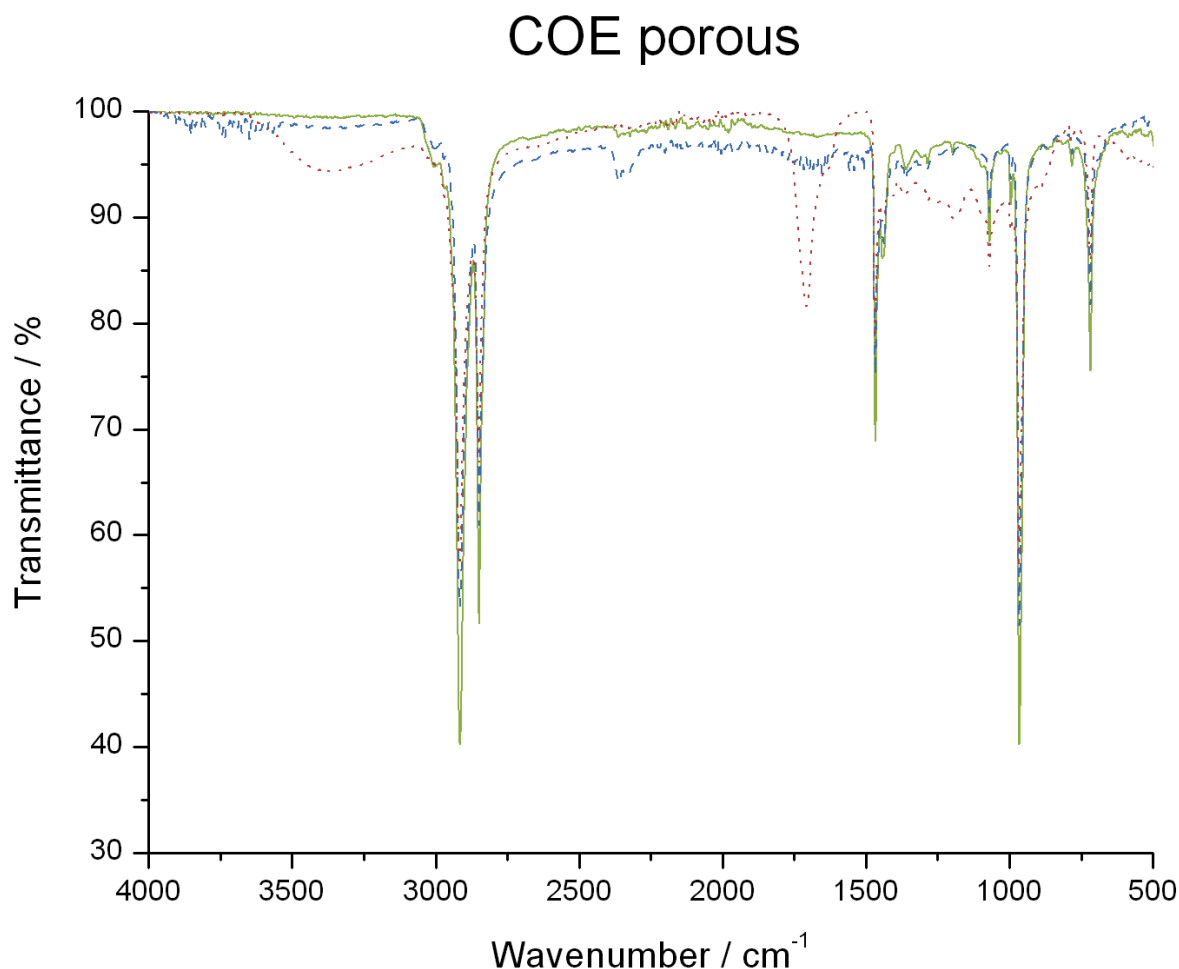


Fig. 30 - FT-IR spectra of porous COE-monolith; green (solid line): unoxidized polyCOE directly after preparation. blue (dashed line): oxidized polyCOE after 14 days. red (dotted line): oxidized polyCOE after 26 days

The unoxidized sample of the porous COE monolith (“porous” in this context stands for the scaffolding-like structure obtained from Synperonic L121) shows the characteristic C-H alkane and alkene C-H stretching vibrations from 3000 - 2780 cm⁻¹ and from 3040 - 3000 cm⁻¹, respectively. C-H scissor vibrations occur at 1480 – 1410 cm⁻¹, resulting from -CH₂- groups from alkanes. Olefinic C=C double bonds show intensive bands with a maximum at 966 cm⁻¹ for the *trans*-C=C- double bond, and another one at 718 cm⁻¹ for the *cis*-isomeres. The proceeding oxidation of the material results in the growth of several characteristic bonds. The O-H stretching vibrations produce a broad signal from about 3600 – 3060 cm⁻¹, which enlarges due to the intermolecular bonding of hydroxyl groups. C=O stretching vibrations arise from saturated and/or α,β -unsaturated ketones. Various signals between 1400 and 1000 cm⁻¹ result from O-H deformation vibrations and C-O stretching vibrations of *secondary* and *tertiary* alcohols.

The increase of the signals, which result from oxidation of the material, is consistent with the data from elemental analysis of the material. The elemental composition of the sample was measured

3. Results and Discussion

directly after preparation (samples were kept under exclusion of oxygen), and 36 days later. Initially, almost no oxygen was found, which is consistent with the data from the IR-spectra (Fig. 30, green line), while the material consists of almost 16 w% oxygen after 36 days (Table 6).

Table 6 - elemental analysis of porous polyCOE monoliths

FPP 108	25.05.2011	10.06.2011	Calcd. for polyCOE
%C	86.78	73.61	87.19
%H	12.57	10.42	12.81
%O	0.65	15.97	0

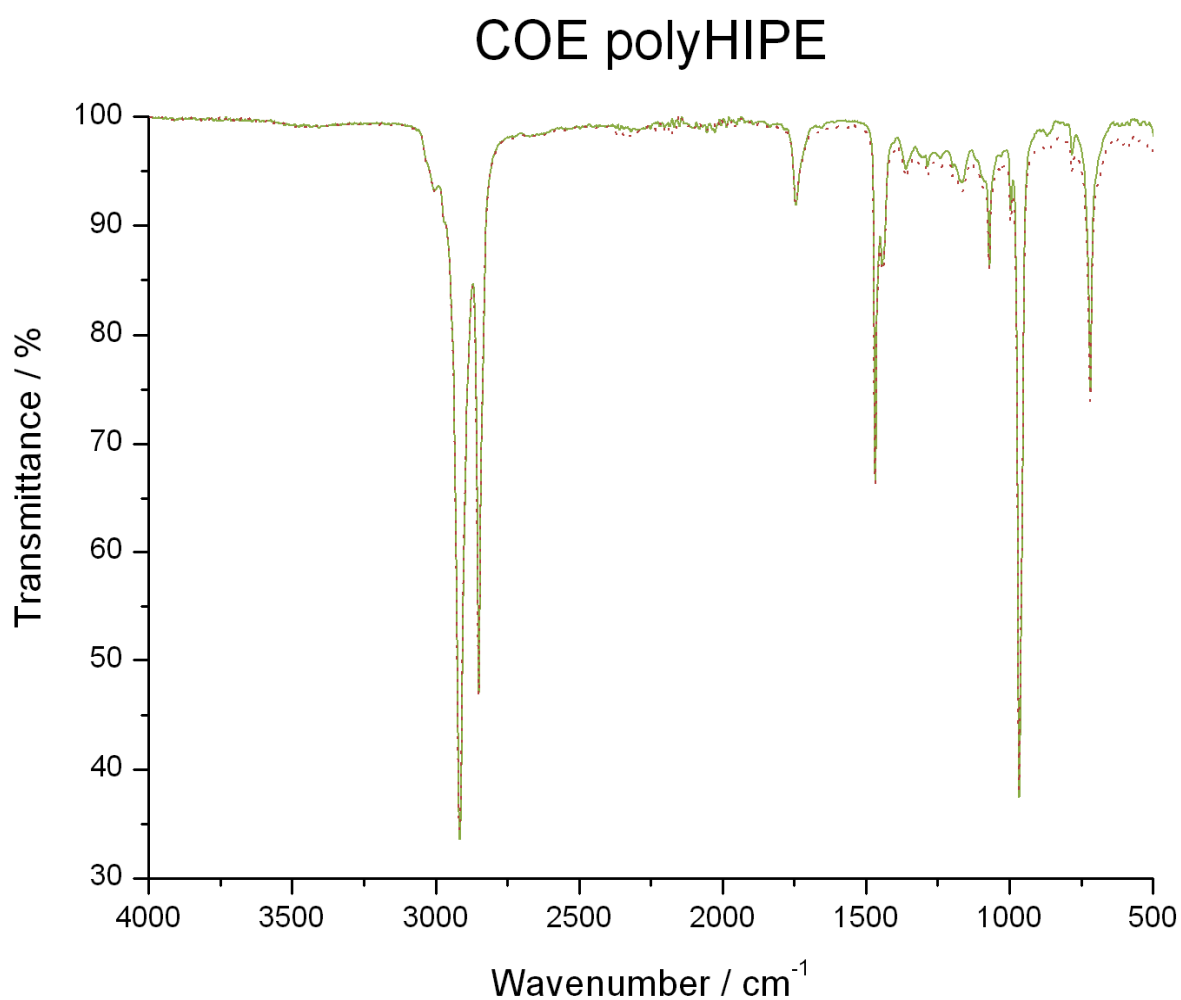


Fig. 31 - FT-IR spectra of COE-polyHIPE; green (solid line): unoxidized polyCOE directly after preparation. red (dotted line): oxidized polyCOE after 26 days

The polyHIPE monolith from cyclooctene does not seem to undergo a strong aging process. The obtained bands result from the aliphatic and olefinic signals from the poly(cyclooctene) backbone.

3. Results and Discussion

The spectrum does not change even after 26 days. The C=O stretching vibration appears from the beginning on, but does not grow further. The region, where peaks from the OH-groups are expected, only shows a very weak signal. The fact that the signals arising from oxidation do not increase brings up the suggestion that the signals could also result from copolymerized surfactant (Span 80). Span 80 possesses hydroxyl groups on its polar head group and an ester bond between the polar head group and the hydrophobic tail. As Span 80 exhibits a double bond in this hydrophobic tail, it could be attached to the polymer chain by olefin metathesis, serving as a chain terminating and/or chain transfer reagent and thus leading to shorter polymer chains. This would give an explanation for the high brittleness of the monoliths prepared with this surfactant.

Elemental analysis confirms the resistance of the polyHIPE to oxidation. Even after 36 days, oxygen comprises only 0.44 w% of the material (Table 7). As no measurement of this monolith was carried out directly after the preparation, there is no information available about the development of the oxygen content.

Table 7 - elemental analysis of the COE polyHIPE

FPP 104	10.06.2011 (36 days on air)	Calcd. for polyCOE
%C	86.93	87.19
%H	12.64	12.81
%O	0.44	0

The resistance of the polyHIPE material to oxidation was surprising, as the scaffolding-like structured monolith has definitely undergone oxidative degradation (vide supra). Scanning electron microscopy of the COE polyHIPE monolith determined open cell morphology (Fig. 29), so that the inner parts of the monolith should be accessible for oxygen. Another very vague assumption is that the polar head of the surfactant protects the subjacent polymer from oxygen. As suggested above, chain transfer reactions could lead to an incorporation of parts of the surfactant. The values measured from the elemental analysis, are almost completely the same as the calculated values from a monolith, where 14.3% of the initially used surfactant are still present in the monolith, maybe due to copolymerization or just because it was not washed out by Soxhlet extraction.

Table 8 - calculated elemental composition of polyCOE with copolymerized surfactant Span 80

1 g COE + 0.021 g Span 80 = 1.021 g total mass		
	mass [g]	w%
%C	0.8860	86.78
%H	0.1302	12.75
%O	0.0047	0.46
total	1.0210	

As only one monolith was measured, this statement remains a rather vague hypothesis, which definitely requires further investigation.

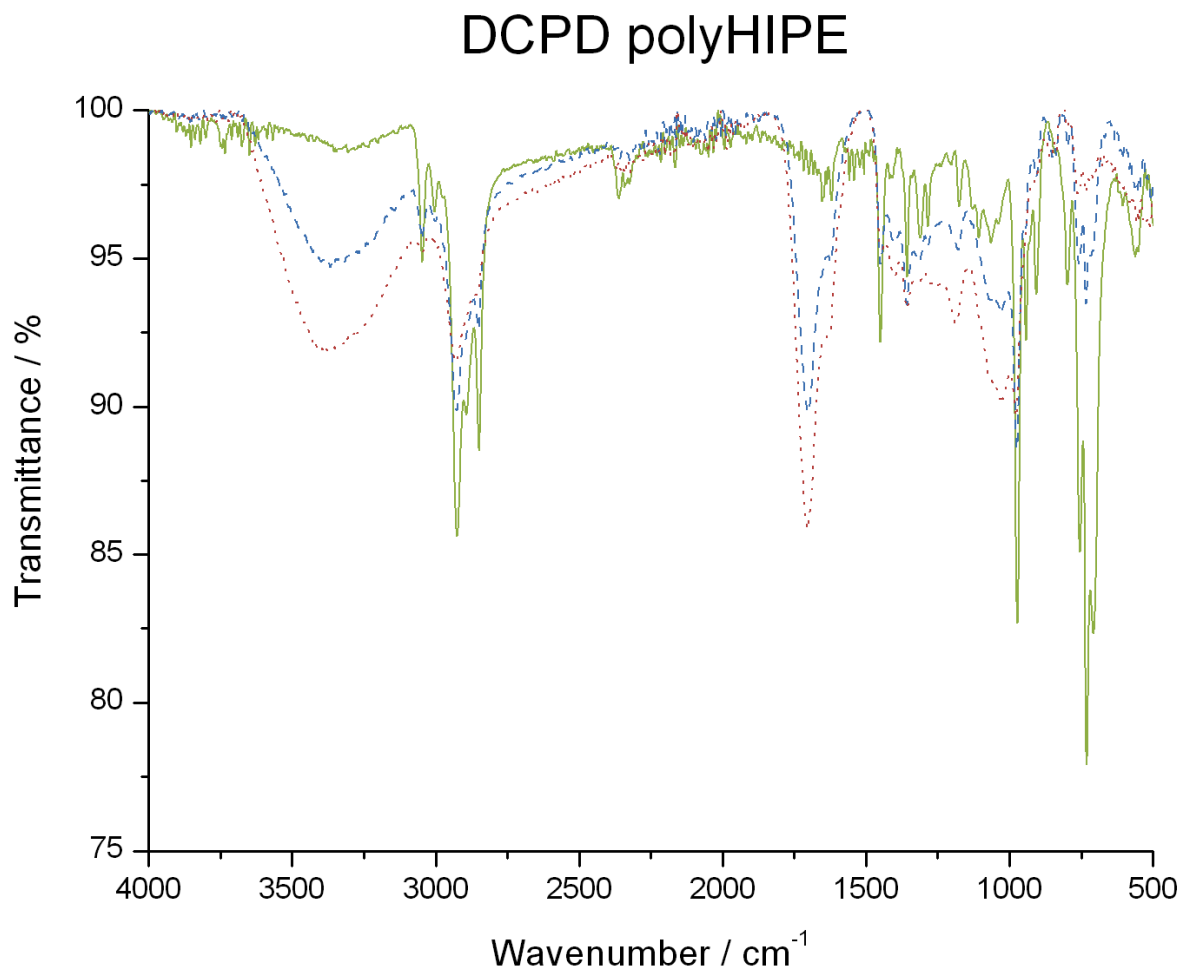


Fig. 32 - FT-IR spectra of DCPD-polyHIPE; green (solid line): unoxidized polyCOE directly after preparation. blue (dashed line): oxidized polyCOE after 10 days. red (dotted line): oxidized polyCOE after 22 days

Compared to poly(cyclooctene), the unoxidized DCPD polyHIPE spectrum shows more alkene C-H stretching vibrations due to the higher content of double bonds. Two maxima appear at 3044 and 3006 cm⁻¹. Interesting is also the intensity of the *cis*- and *trans*-C=C signals with maxima at 755, 730 and 705 cm⁻¹ for *cis*- and 975 for *trans*-C-H deformation vibrations, whereat the *cis*-signal at 705 cm⁻¹ refers to the unreacted cyclopentene-ring of DCPD.⁴¹ In contrast to observations in polyCOE, in polyDCPD, the *cis*-signal is stronger than the *trans*-signal. Aging of the material does not only decrease signals from C=C double bonds, but also aliphatic vibration signals. Hydrogen abstraction from C-H bonds in allylic positions is considered a probable reason for this observation, as plenty of *tertiary* C-

3. Results and Discussion

H bonds that are present in polyDCPD are weaker compared to *secondary* ones, thus reacting easier and faster with oxygen.

Elemental analysis confirms the rapid oxidation of polyDCPD. After 5 weeks of exposure to air and sunlight, more than 31% of the material consists of oxygen, which is close to the maximum value of 32%.⁴²

Table 9 - elemental analysis of the DCPD polyHIPE

FPP 114	25.05.2011	10.06.2011	Calcd. for polyDCPD
%C	73.35	62.07	90.85
%H	7.41	6.65	9.15
%O	19.23	31.27	0

In summary, infrared measurements show that polyHIPEs from DCPD are more sensitive to oxygen than their COE pendants. The monoliths from DCPD oxidize rapidly, indicated by the color change from white to yellow and increasing brittleness of the samples. The results from IR-spectroscopy are confirmed by elemental analysis, which determined an almost complete oxidation of polyDCPD within five weeks. Also the scaffolding-like, porous polyCOE monoliths undergoes rapid aging, while the COE polyHIPE is almost completely resistant. The latter observation cannot be explained properly yet, and requires further investigation.

It is well known that bulk material of polyDCPD usually passivates due to formation of a highly polar, oxidized surface layer, which protects the subjacent material from further oxidation; a familiar process known from aluminum. However, investigations of such a passivated, protective layer of oxidized polyDCPD usually exhibit a thickness ranging from 4-20 μm , depending on the aging conditions.⁴³ As the walls of polyHIPE material usually possess a thickness of less than 1 μm , it can be assumed that oxygen penetrates the entire material and completely oxidizes the polymer, which is consistent with the results presented above.

3.4. Co-polymerization of DCPD and COE

Random copolymers of dicyclopentadiene and cyclooctene were synthesized to investigate the effect of incorporating linear COE-chains to the crosslinked DCPD-network. Starting with pure DCPD, the COE content was increased stepwise up to 50 mol% for each sample. Emulsions with an internal phase ratio of 80% were prepared with Synperonic L121 as this surfactant gave polyHIPE structure using pure DCPD. The reaction mixtures with incorporated initiator (M2) were separated in two glass molds and cured for 30 min and 1h respectively, followed by acetone extraction and vacuum drying

3. Results and Discussion

of the obtained monoliths. Due to the fast polymerization of DCPD, the initiator loading was reduced to 4000:1 (molar ratio of monomer to initiator).

Interestingly, the monoliths with increasing COE content shrank upon vacuum drying. Selected samples were analyzed by scanning electron microscopy to determine the morphology of the porous samples (SEM images were taken from samples cured for 30 min, as no difference in the morphologies is expected due to a slightly longer curing time).

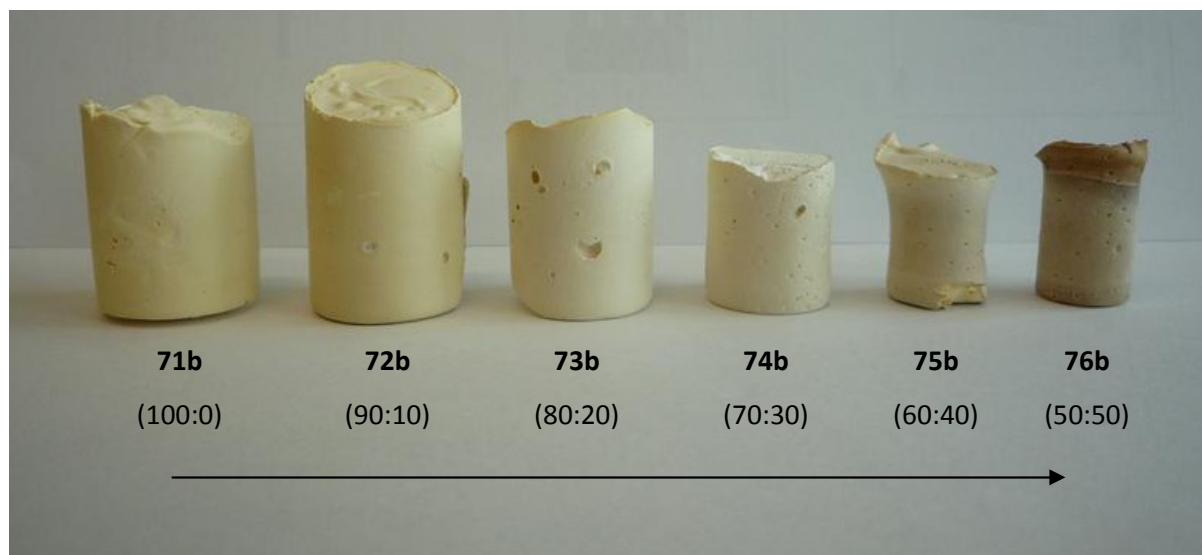


Fig. 33 - DCPE-COE co-polyHIPEs with increasing COE concentration (values in brackets indicate molar ratios of DCPD:COE). pictured samples were cured for 1h at 80°C

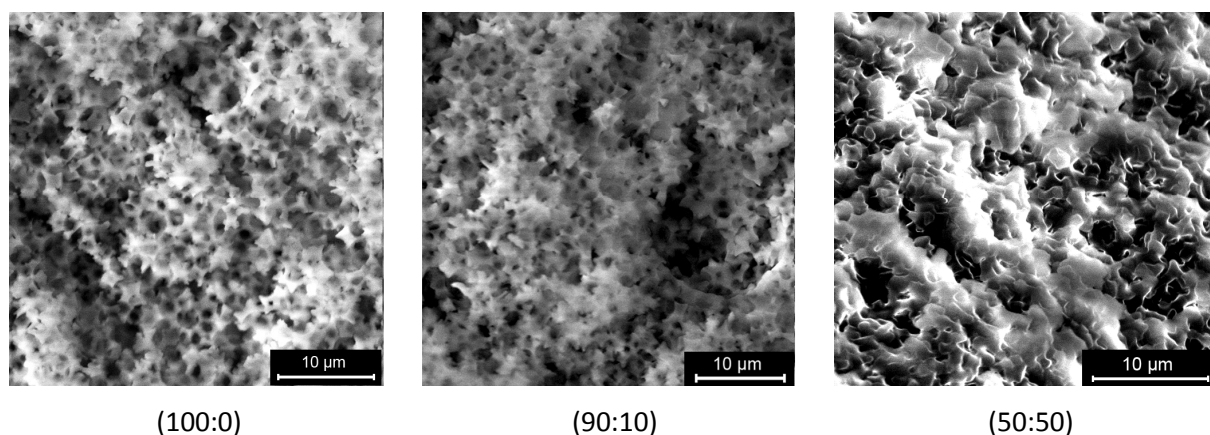


Fig. 34 - Scanning electron microscopy images of co-polyHIPEs from DCPD and COE

The sample prepared from pure DCPD and the one with 10 mol% COE exhibit polyHIPE morphology (Fig. 34. left and middle image; the poor image quality results from the measurements in low vacuum mode). The monolith with 50% DCPD and COE each does not possess polyHIPE structure.

Instead, a worm-like structure was obtained, resembling the one obtained from pure DCPD with Span 80. This is again a proof that Synperonic L121 and cyclooctene do not form stable W/O emulsions under these conditions. The increasing amount of COE seems to destabilize the emulsion. The loss of polyHIPE structure goes hand in hand with shrinking of the monolith after extraction and vacuum drying: the 50:50 mixture shrank to almost half of its original size (see Fig. 34: the pure DCPD monolith remained in its initial form given from the mold, while the 50:50 mixture on the right shrank drastically). The former internal phase stabilizes the polymer-scaffolding until it is removed, resulting in a collapse of the structure.

The collapsed monoliths also show an interesting “core-shell” structure (Fig. 35 - “core-shell” structure of collapsed monoliths). The white color indicates porosity of the internal part, while the outer shell became transparent. The samples were cured in an oven, so that they heat from outside in. This suggests that the emulsion undergoes a faster phase separation in outer regions than in the internal part, thus preserving a porous morphology in the core, while the shell consists of bulk polymer. However, this suggestion was not proven by scanning electron microscopy so further investigations are required to give evidence about this issue.



Fig. 35 - “core-shell” structure of collapsed monoliths (sample 76b, 50:50 copolymer)

Maybe, upon increasing content of DCPD, the high amount of crosslinking sites results in a tightening of the elastic COE chains, which are rearranging and forming ravel, thus shrinking the material occurs.

Due to the instability of the emulsion, no feasible co-polyHIPEs with high cyclooctene amounts could be prepared. Interestingly, the shrinking was not observed in earlier preparations, when only 5% of DCPD were copolymerized with COE (e.g FPP23-I).

3.5. Preparation of shouldered test bars and mechanical testing of porous polycyclooctene

The mechanical properties of the prepared materials were tested for tensile strength to determine the Young’s moduli. The high brittleness of the COE polyHIPEs made it impossible to prepare shouldered test bars. However, the material from emulsions with Synperonic L121 was investigated. Emulsions were prepared in the same way as for the monoliths, and transferred to a pre-heated steel mold. The pre-heating was necessary to obtain solid material upon curing for 30 minutes. Earlier approaches with cold molds did not lead to a solid material. The polymerization was either too slow due to the slow heating of the massive steel mold, or decomposition of the material occurred, when

3. Results and Discussion

the emulsion was cured for too long. Successfully polymerized test bars were rinsed with acetone and put in a bowl with acetone to extract the surfactant and the water. After vacuum drying, white, soft test bars were obtained (Fig. 36).

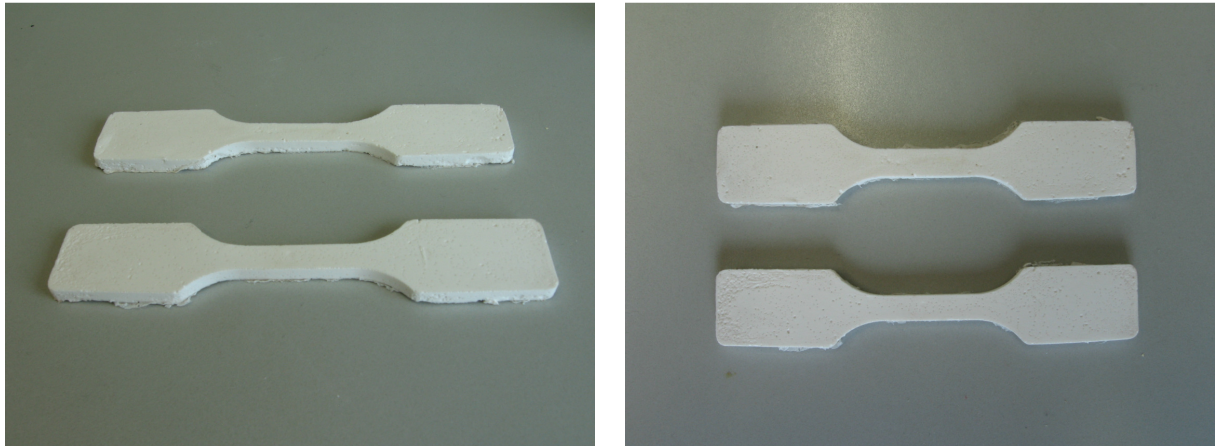


Fig. 36 - shouldered test bars for tensile strength tests

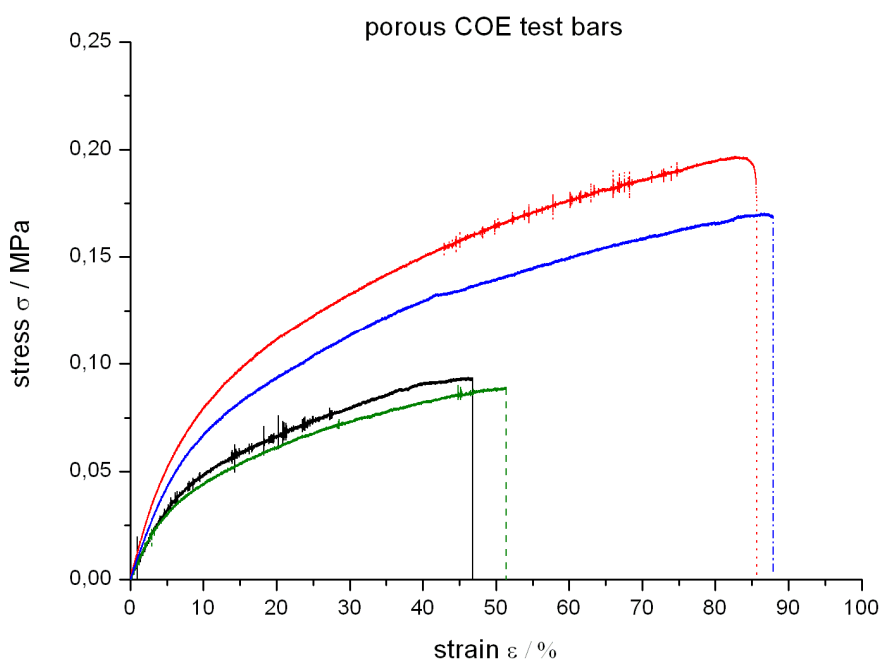


Fig. 37 – tensile strength measurements of porous COE test bars; 4 bars measured (FPP111, 118b, 120a, 120b)

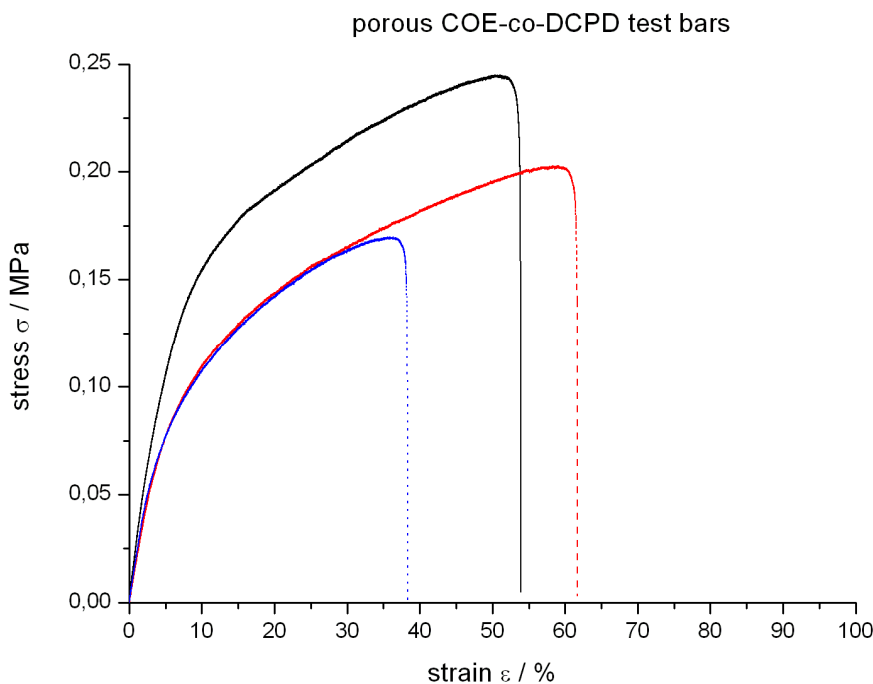


Fig. 38 – tensile strength measurements of porous COE-co-DCPD test bars, 3 measurements (FPP121, 122a, 122b)

The Young's moduli were calculated from the initial linear slope of the strain/stress plot. Nominal stress (σ_M) and nominal strain (ϵ_M) represent the values at break.

Table 10 – Young's moduli (E), nominal strain (ϵ_M) and nominal stress (σ_M) of test bars

sample	E [MPa]	ϵ_M [%]	σ_M [MPa]
FPP111	0.74	46.86	0.09
FPP113	0.73	51.38	0.09
FPP118a	1.19	85.27	0.19
FPP118b	0.87	87.95	0.17
\bar{x}	0.88		
FPP121	2.62	53.47	0.23
FPP122a	1.81	61.44	0.19
FPP122b	2.11	37.85	0.16
\bar{x}	2.18		

The tensile tests have shown a very low Young's modulus for porous cyclooctene ranging from 0.74 to 1.19 MPa, and a maximum elongation up to 88%. Anyway, these results are not surprising, as the polymer consists only of linear chains with weak interactions from van der Waals forces and possible entanglement of macrocycles. The incorporation of DCPD led to an increase of the elasticity modulus for almost 150% due to crosslinking of the poly(cyclooctene) chains. However, the increase is very low considering the incorporated amount of crosslinker (5 mol%). The higher reactivity of

DCPD compared to COE may have led to an accumulation of crosslinking sites in the polymer network instead of a uniform distribution, leading to a reduced reinforcement of the material. The high variance of the values can have several reasons. First of all, the preparation process was not very easy, as many factors had an influence on the solidification of the material, mainly the temperature of the mold before the emulsion was poured in, and the temperature of the oven itself, which was often very inconstant. Another point is the extraction of the internal phase and the surfactant, which was carried out by inlaying the test bars in acetone for several hours. The time for this procedure, as well as the frequency how often the acetone was changed was not kept constant. Soxhlet extraction was not possible, as the test bars deformed overnight on vertical placement. Also the way how the bars were clamped into the tensile testing machine can have a big influence on the values. As the test bars were very soft, they usually deformed slightly, when they were fixed, so the measurements were not very accurate. To reduce the variance, more measurements and a standard workup procedure are suggested.

3.6. The surfactant mystery

Synperonic L121, a (poly(ethylene glycol)-block-poly(propylene glycol)-block-poly(ethylene glycol) triblock copolymer was used for the preparation of emulsion templated porous poly(cyclooctene), giving rise to a scaffolding-like 3-dimensional polymer network, as reported in section 3.1. The surfactant was purchased from Sigma-Aldrich, and used as received. As it was used up, a new bottle should be ordered, as we noticed that the product was switched from Synperonic L121 (trademark of Unichema Chemie BV) to Pluronic L121 (trademark of BASF Corporation). Both surfactants were described as PEO-PPO-PEO surfactants with an average molecular weight of 4,400 g/mol, so Pluronic L121 was purchased and used as received. Numerous attempts were accomplished, but the porous structures could not be reproduced, and not even any solid monolithic material was obtained. Switching back to Synperonic L121, which was provided from our colleagues from the University of Maribor, monoliths could be prepared again from the first try on. Investigations on the surfactant did not show any difference in NMR spectra, suggesting that there was no difference in the chemical composition of the surfactants. However, GPC (Gel Permeation Chromatography) has shown a discrepancy in the distribution of the surfactant's molecular weight. In Fig. 39, all GPC measurements are presented, showing all four samples of the "L121 – series" from different sources; the fourth sample was a gift from Croda France, former Unichema Chemie BV.

GPC-data were normalized to a maximum value of one, for the highest molecular weights, to equal concentration differences of the measurements. The peaks of all four surfactants appear around 28.5 mL retention volume (retV), whereat Pluronic L121 (BASF SE) has the highest molecular

weight with about 8450 g/mol relative to poly(styrene) standards. Both Synperonic L121, which could be successfully employed for monolith preparation, show a similar M_w of 7850 and 7900, respectively. Synperonic PE/L121 from Croda France has the lowest molar weight of only 7300 g/mol. Besides the differences in the main peaks, there is an obvious discrepancy at lower molecular weights. Both employed Synperonic L121 exhibit a high amount of smaller fractions at about 30 mL retV, representing a M_w of 4000 g/mol. All four surfactants possess small molecular weight fractions, ranging from about 4000 – 800 g/mol, but the amount is much higher in the two Synperonic L121, than in Pluronic L121 and the Synperonic PE/L121 from Croda France.

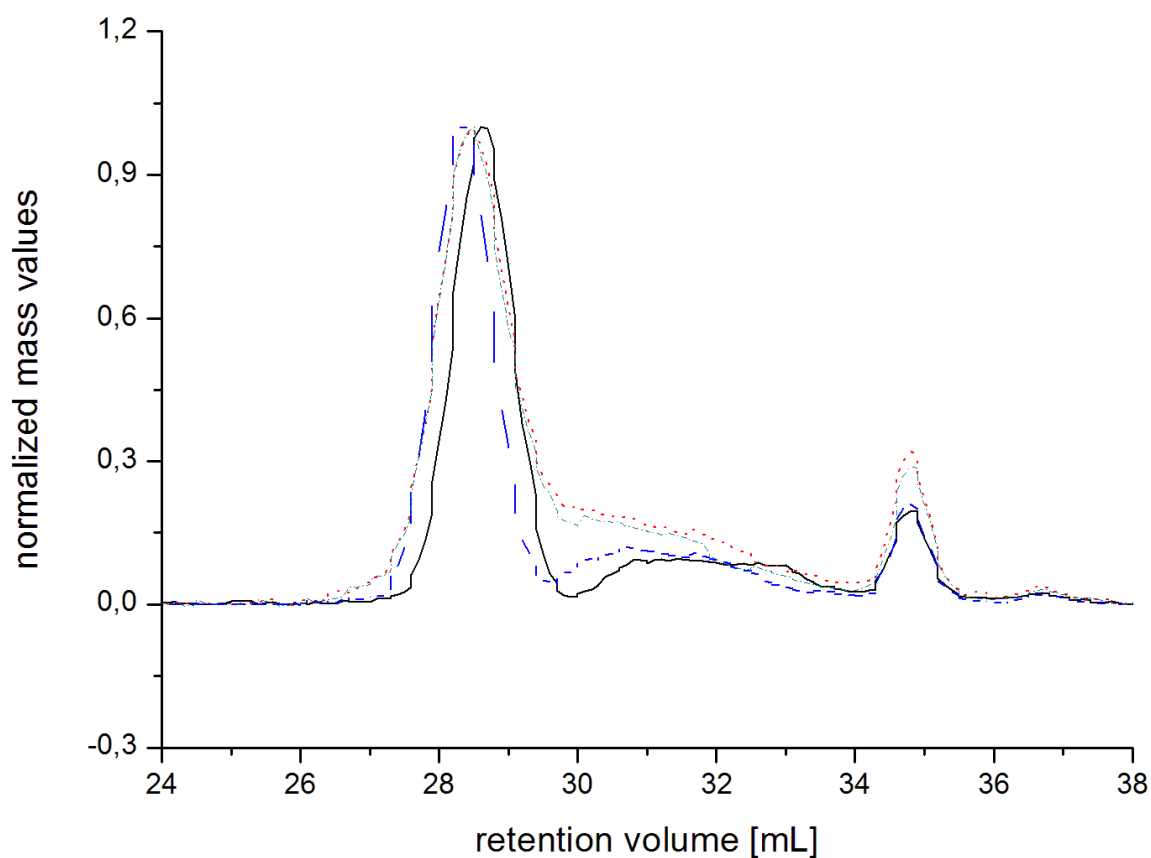


Fig. 39 – normalized refractive index chromatogram of different "L121" surfactants - red line (dotted): Synperonic L121 (1st attempts, successful preparation of porous monoliths, Unichema Chemie BV); green line (dashed-dotted line): Synperonic L121 (2nd attempts, again successful preparation of solid monoliths, Unichema Chemie BV); black (solid line): Pluronic L121 (BASF – no solidification of the emulsion); blue (dashed line): Synperonic PE/L121 (Croda France, not yet tested)

The impossibility of preparing solid monoliths from Pluronic L121 may be ascribed to the instability of water/cyclooctene emulsions prepared from this surfactant. The appearance of low molecular weight fractions in the Synperonics from Unichema Chemie BV suggests that these smaller molecules act as co-surfactants, thus producing more stable emulsions.

4. Conclusion and Outlook

The target of preparing polyHIPE structured monoliths from cyclooctene has been reached and the synthesis was successfully demonstrated within this work. An inherently reactive system was developed allowing the preparation of polyHIPEs at ambient conditions, due to the high reactivity of M20 at room temperature. Span 80 was demonstrated to be a proper surfactant for obtaining stable W/O emulsions at low, as well as at higher temperatures of 80°C, thus polyHIPE morphology was preserved in the solid material. However, a significant drawback of the obtained material is a pronounced brittleness, making further use and functionalization difficult. Reinforcement of the material via crosslinking with DCPD did not significantly improve the mechanical properties of the material.

The employment of Synperonic L121 as stabilizer did not result in a polyHIPE structure. Emulsion instability resulted in the formation of a scaffolding-like, 3-dimensional structure upon polymerization, yet solid, elastic monoliths were obtained. Mechanical testing (tensile strength) determined low Young's moduli of about 1 MPa and a considerable elasticity up to 90% elongation. Incorporation of 5 mol% DCPD in the COE material more than doubled the Young's moduli due to crosslinking of the polymer, while at the same time reducing the maximum elongation of the material.

Copolymerization of DCPD and COE was found to be difficult due to the incompatibility of cyclooctene with Synperonic L121 and - vice versa - of DCPD with Span 80. Upon incorporation of COE to W/O emulsions of DCPD, stabilized with Synperonic L121, the polyHIPE morphology was lost at values of about 20-30 mol% of COE, which was accompanied by shrinking of the monoliths after extraction and vacuum drying.

The long term stability of porous cyclooctene derived materials has also been investigated via FT-IR measurements and elemental analysis, exhibiting a slower aging of poly(cyclooctene) compared to polyDCPD. To overcome the brittleness of the COE-polyHIPE monoliths, other surfactants with saturated hydrocarbon tails are recommended to be tested, as the double bond of Span 80 is considered to interact with the initiator by metathesis, acting as a chain termination reagent. Nevertheless, the oxidation stability of poly(cyclooctene) is a clear advantage compared to polyDCPD. However, a general investigation on lowering the oxidation susceptibility of ROMP-derived materials is recommended, e.g. by hydrogenation of the double bonds.

Further exploration of ROMP as a tool in this area of material science should be carried out, as the target of functionalization was not yet reached within this thesis. However, the promising functionalization possibilities reported above strongly suggest further ambition towards ROMP-derived polyHIPE materials.

5. Experimental section

5.1. Reagents

Chemicals and solvents were purchased from commercial sources (Sigma Aldrich, Roth Chemikalien) and used as received without further purification. ROMP Initiators M2, M31, M51 and M20 were purchased from Umicore Precious Metals AG and used as received.

5.2. Instruments

Scanning Electron Microscopy (SEM)

Scanning Electron Microscopy was carried out on a Quanta200 3D microscope, using a tungsten cathode as electron source. High and low vacuum measurements were recorded with a large field gaseous secondary electron detector (LF-GSED). Magnifications ranging from 100X to 20.000X were achieved using a voltage between 3 - 20 kV. The sample preparation included breaking in liquid nitrogen followed by gold plating.

FT-IR Spectroscopy

FT-IR spectra were recorded on a Bruker Alpha-P infrared spectrometer, equipped with an attenuated total reflection (ATR) accessory using a diamond crystal.

Elemental Analysis

Elemental composition was measured with a Universal-Elementaranalysator Vario El III, determining the C, H and N content. The oxygen content was calculated as the residual weight to 100% weight loss.

Mechanical testing

Tensile strength tests were done on a Shimadzu Autograph AGS-X, with a force measuring range from 10-10kN. Clamping length of the samples was 8 cm; no initial tension was applied. The area of the shouldered test bars was 42.5 mm² in the reduced section; samples were measured with a speed of 1 mm/min.

Simultaneous Thermal Analysis (STA)

STA was carried out on a Netzsch 449C apparatus, using helium as purge gas. Thermogravimetric losses were monitored up to a temperature of 550°C applying a heating rate of 10°C/min.

5.3. Preparation of porous polymers

5.3.1. Porous monoliths

5.3.1.1. FPP20

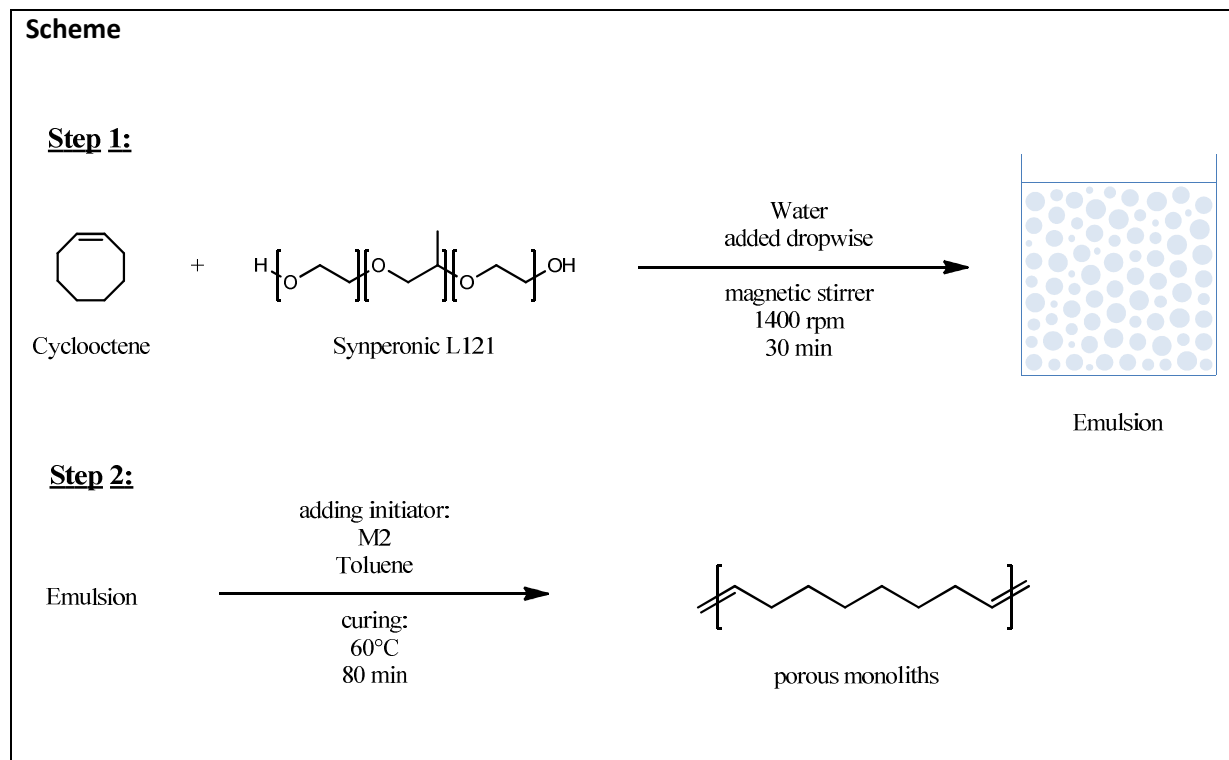


Table 11 - reactants for reaction FPP20/22

	COE		Synp.L121	H ₂ O	M2		toluene	M2 : COE
	m [g]	n [mol]	m [g]	V [mL]	m [mg]	w%	V [μL]	
I	1.0168	9.23E-03	0.1479	4.4	1.0	0.1	1.05E-06	200 1 : 8757
II	0.9948	9.03E-03	0.1463	4.4	2.0	0.2	2.11E-06	200 1 : 4284
III	1.0300	9.35E-03	0.1475	4.4	3.0	0.3	3.16E-06	200 1 : 2957
IV	0.9993	9.07E-03	0.1463	4.4	4.0	0.4	4.21E-06	200 1 : 2152
V	1.0184	9.24E-03	0.1416	4.4	5.0	0.5	5.27E-06	200 1 : 1754

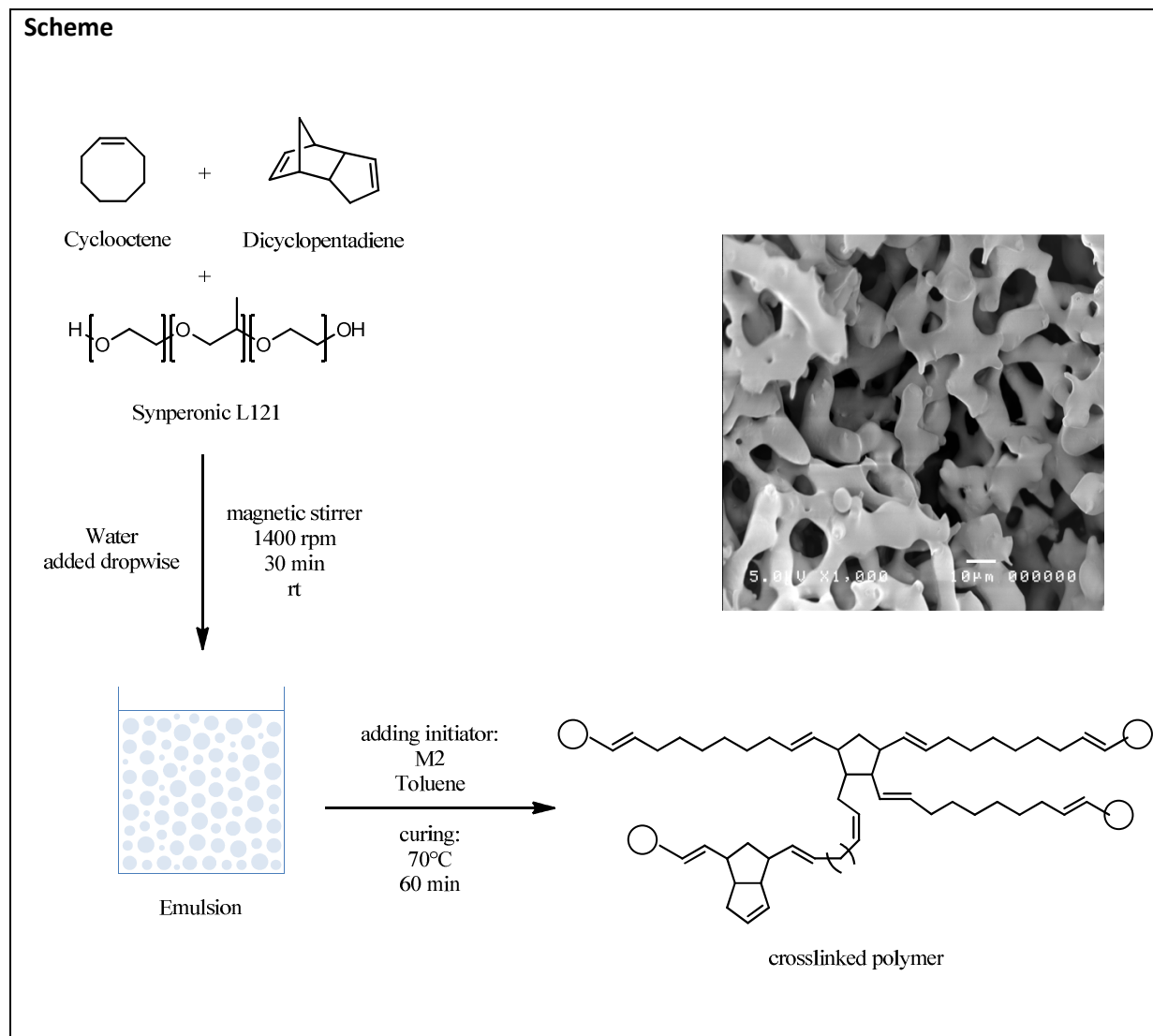
Procedure

Five different samples with varying initiator loadings were prepared according to Table 11. A magnetic stirrer was used instead of an overhead stirrer, and the emulsion was prepared in small 20 mL glass vials. The initiator was added to the mixture which was then homogenized cured directly in the vials. After curing (60°C, 80 min) the samples became grey showing different consistencies. Sample I had a firm skin on top but was creamy inside. Sample II was soft inside but inherently stable. The monoliths III, IV and V were a little tougher, more solid than II. and there was no noticeable difference between them.

5. Experimental section

The samples were directly dried in the vials in vacuo, what led to a deformation of the monoliths due to the uncontrolled boiling of the water under reduced pressure. Sample III was then taken out from the glass vial, and extracted with acetone in a soxhlet. After the extraction a white monolith was obtained. Subsequent vacuum drying led to a further solidification of the material, resulting in an elastic monolith. Samples I,II,IV and V were not further extracted and dried.

5.3.1.2. *FPP23-I*

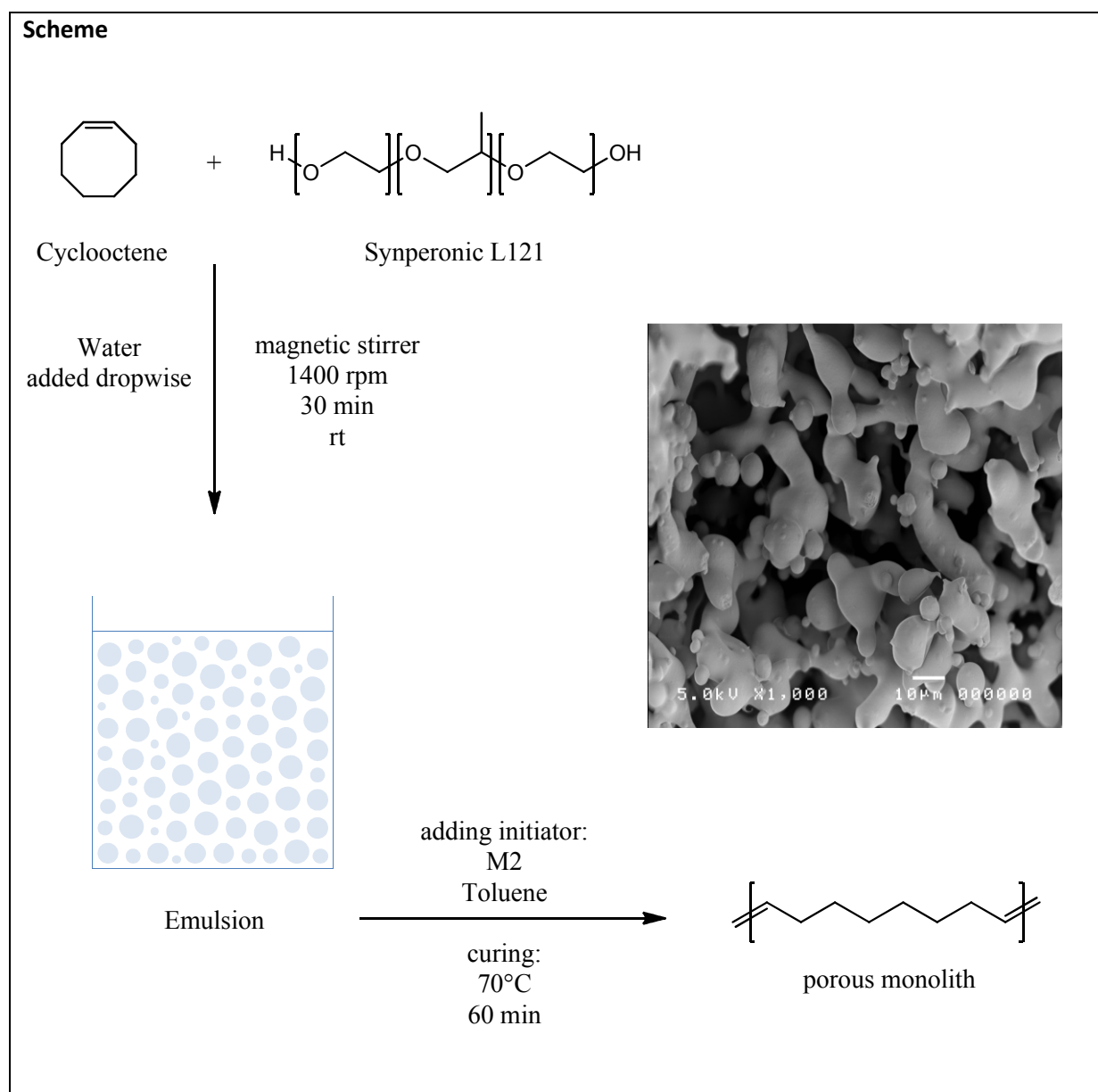


5. Experimental section

Table 12 - reactants for reaction FPP23-I

	M [g/mol]	m [g]	n [mol]	V [mL]	ρ [g/mL]
cyclooctene	110.20	1.001	9.08E-03		0.8500
DCPD	132.20	0.049	3.71E-04		0.9800
Synperonic L121	4400.00	0.14360	3.26E-05		
water	18.02			4.4	
M2	949.09	3 mg	3.16E-06		
toluene	92.14	0.1746	1.89E-03	0.2	0.8730
monomer : initiator	2991				
porosity [%]:	78.92				

5.3.1.3. *FPP23-II*



5. Experimental section

Table 13 - reactants for reaction FPP23-II

	M [g/mol]	m [g]	n [mol]	V [mL]	ρ [g/mL]
cyclooctene	110.20	1.01	9.17E-03		0.8500
Synperonic L121	4400.00	0.15350	3.49E-05		
water	18.02			4.4	
M2	949.09	3 mg	3.16E-06		
toluene	92.14	0.1746	1.89E-03	0.2	0.8730
monomer : initiator	2900				
porosity [%]:	78.8				

Procedure

The emulsions were prepared as reported above for FPP20; using amounts according to Table 12 for FPP23-I and Table 13 for FPP23-II. After the initiator solution was added and homogenized, the reaction mixture was transferred to 20 mL glass vials, sealed with a cap and cured in an oven at 70°C for 1h. The monoliths were extracted with acetone in a soxhlet overnight, followed by vacuum drying.

Analysis

Simultaneous Thermal Analysis (STA):

sample	Melting point [°C]
FPP23-I	74.2
FPP23-II	69.6

5.3.1.4. *FPP28*

sample	COE	Synp. L121	Span 80	H₂O	DCM
	V [mL]	m [g]	m [g]	V [mL]	V [μL]
I	1.0190	0.1557	-	4.4	200 μ L
II	1.0081	0.3026	-	4.4	200 μ L
III	1.0018	0.2060	-	4.4	200 μ L
IV	1.0080	-	0.1450	4.4	200 μ L
V	1.0137	-	0.2979	4.4	200 μ L
VI	1.0066	-	0.2010	4.4	200 μ L

Procedure

Surfactant and COE were put in a 20 mL glass vial and stirred with a magnetic stirrer at about 400 rpm. Water was subsequently added dropwise with a pipette and the stirring speed was slowly raised to 1400 rpm. After addition of water, the mixtures were stirred for 1h at 1400 rpm. The samples were left overnight at room temperature to determine emulsion stability. As no phase separation

5. Experimental section

was observed, 200 μL of DCM were added and incorporated into the solution to determine the effect of the catalyst solvent on emulsion's stability. The samples were then put into an oven at 60°C to simulate curing conditions and to study whether phases would separate.

5.3.1.5. *FPP29*

	COE		Span 80	H ₂ O		M2		DCM	M2:COE
	V [mL]	n [mol]	m [g]	V [mL]	m [mg]	w%	n [mol]	V [μL]	
a	1.0102	9.17E-03	0.1531	4.4	1.0	0.1	1.05E-06	200	8700
b	1.0050	9.12E-03	0.1640	4.4	2.0	0.2	2.11E-06	200	4328
c	1.0047	9.12E-03	0.1561	4.4	3.0	0.3	3.16E-06	200	2884
d	1.0087	9.15E-03	0.1501	4.4	4.0	0.4	4.21E-06	200	2172
e	1.0071	9.14E-03	0.1469	4.4	5.0	0.5	5.27E-06	200	1735
f	0.9970	9.05E-03	0.16320	4.4	2.0	0.2	2.11E-06	200	4293

Procedure

Span 80 and COE were put in 20 mL glass vials, water was added dropwise with a pipette under stirring at 400 rpm. The stirring speed was slowly raised to 1400 rpm and the mixture was further stirred for 1h 5 min after complete addition of the internal phase. M2 was dissolved in DCM and incorporated into the emulsion. Samples a)-e) were cured in an oven at 60°C, f) at room temperature. After 15 minutes, bubbles with a diameter of about 1-2 mm were formed (evaporating DCM). The samples were removed from the oven after 60 min. Sample a) did not solidify and gave a creamy substance; b) gave a soft, but not solid material; c)-e) were solid, but very brittle. Sample f) did not give a solid monolith, but the mixture polymerized a little and gave a cloggy mixture.

5.3.1.6. *FPP30*

sample	COE		DCPD		Span 80	H ₂ O	M2		M2 : MM
	V [mL]	n [mol]	V [mL]	n [mol]	m [g]	V [mL]	m [mg]	n [mol]	
a	1.0134	9.20E-03	-	-	0.2028	4.4	3.0	3.16E-06	2909
b	1.0003	9.08E-03	-	-	0.2201	4.4	5.0	5.27E-06	1723
c	0.9491	8.61E-03	0.0583	4.41E-04	0.1965	4.4	3.0	3.16E-06	2864
d	0.9570	8.68E-03	0.1142	8.64E-04	0.1925	4.4	5.0	5.27E-06	1812
e	-	-	0.9995	7.56E-03	0.1866	4.4	1.0	1.05E-06	7176
f	-	-	1.0000	7.56E-03	0.2056	4.4	2.0	2.11E-06	3590

5. Experimental section

Procedure

The sample preparation was carried out as for reaction FPP29 above, however DCM was replaced by toluene. After curing the samples for 15 min at 60°C sample e) and f) were inherently stable and did not flow any more upon tilting the mold. Sample a) and b) were still viscous. After 45 min e) and f) were almost solid, and the cap from the mold was removed to dry the samples (evaporate the internal phase). After 1h 30 min. the samples a)-d) were removed from the oven, while e) and f) were dried over the weekend. While e) and f) solidified, the other samples did not give solid monoliths, but a semisolid, cloggy mixture. After 64h, e) and f) were removed from the oven, and the monoliths had a dark yellow color.

5.3.1.7. FPP32

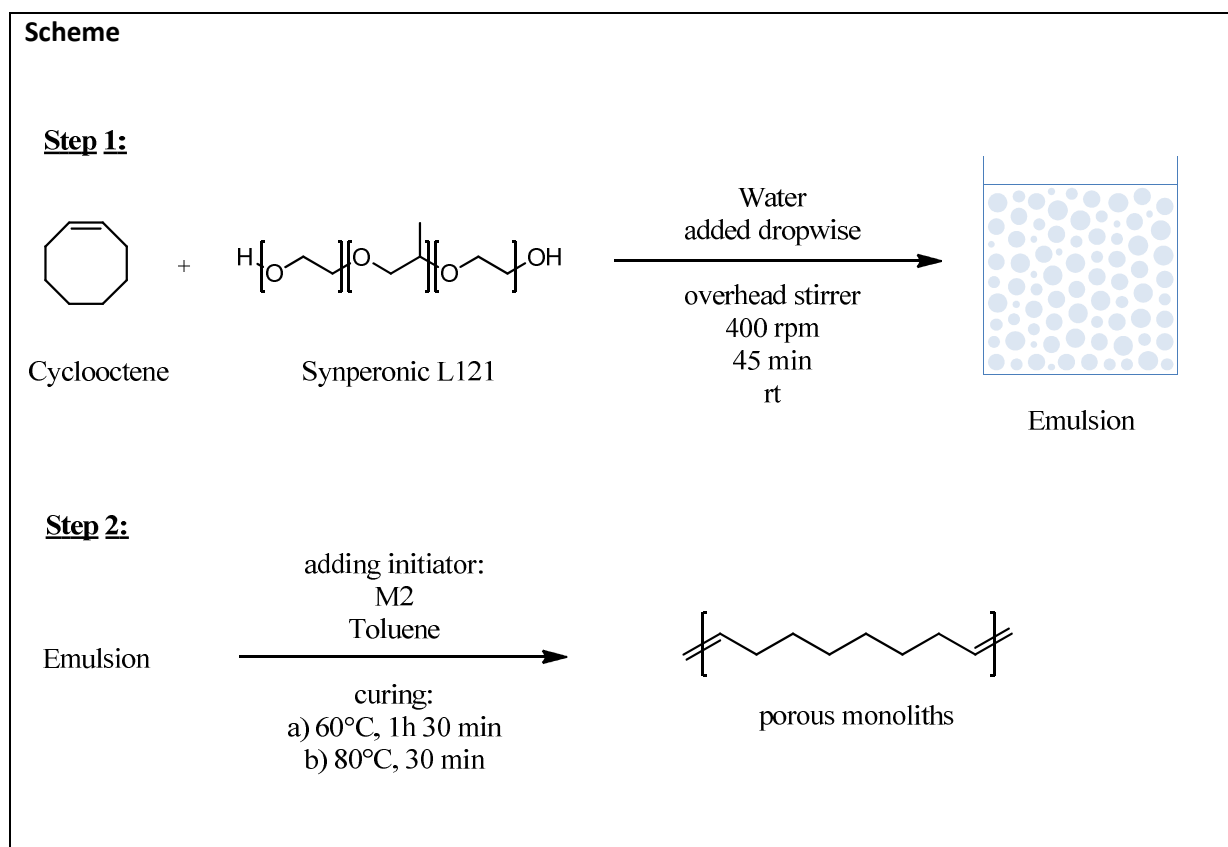


Table 14 - reactants for reaction FPP32

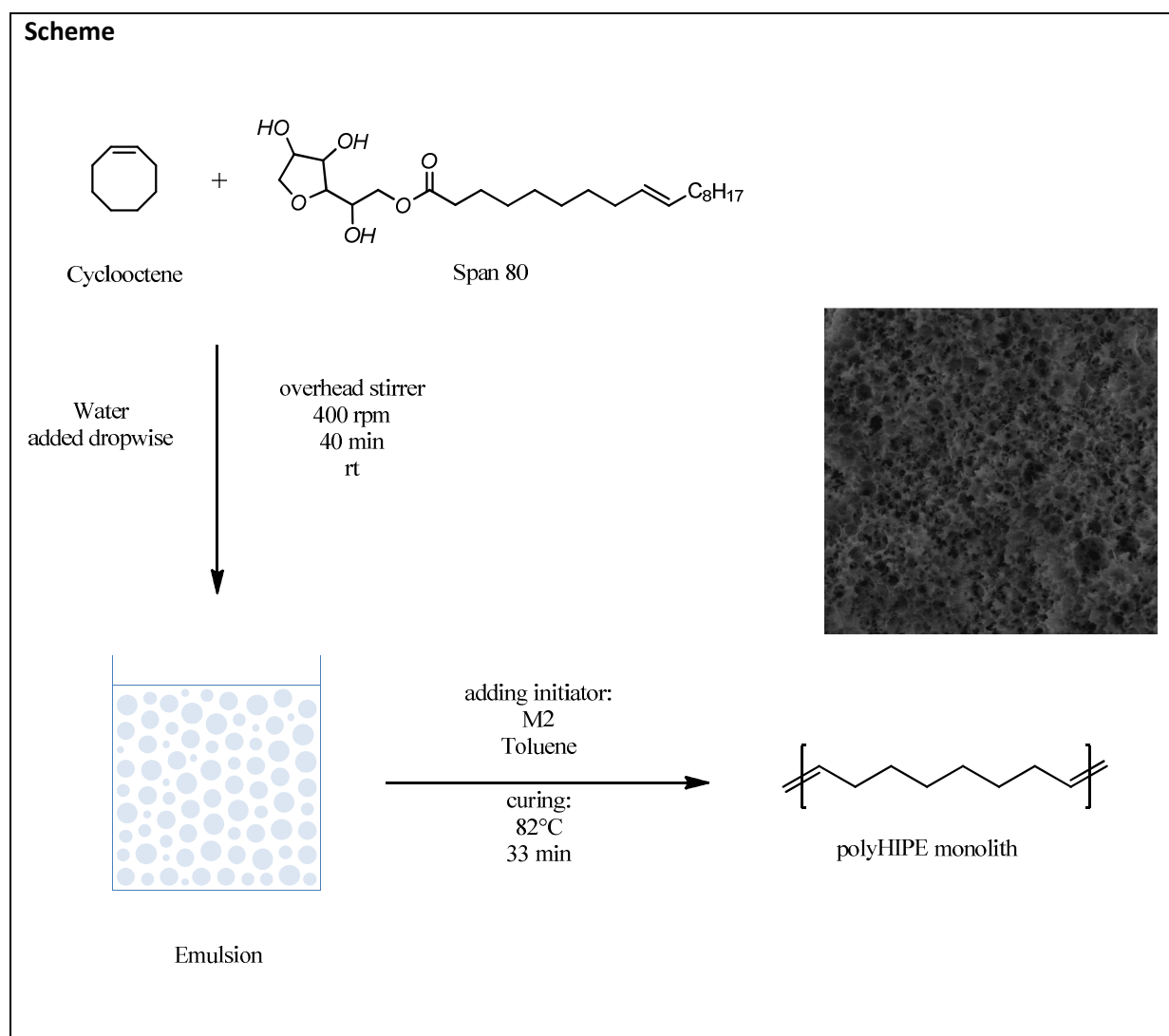
	M [g/mol]	m [g]	n [mol]	V [mL]	ρ [g/mL]
cyclooctene	110.20	10.0044	9.08E-02		0.8500
Synperonic L121	4400.00	1.4985	3.41E-04		
water	18.02			47	
M2	949.09	29.0	3.06E-05		
toluene	92.14	1.5714	1.71E-02	2	0.8730
monomer : initiator	2971				
porosity [%]:	80.00				

5. Experimental section

Procedure

The emulsion was prepared as described in the general procedure with an overhead stirrer. After adding the initiator and subsequent homogenization, the mixture was divided and transferred to two polypropylene molds. One sample was cured at 60°C for 1h 30 min (a) and the other one at 80°C for 30 min (b). After curing, the samples were cooled down to room temperature and left in the mold for 1-2h to stabilize the structure. Subsequent extraction with acetone and vacuum drying gave two white, solid monoliths.

5.3.1.8. *FPP55*



5. Experimental section

Table 15 - reactants for reaction FPP55

	M [g/mol]	m [g]	n [mol]	V [mL]	ρ [g/mL]
cyclooctene	110.20	4.51070	0.04093		0.8500
Span 80	428.60	0.90300	0.00004		
water	18.02	22.00000			
M2	949.09	38.85 mg	0.00004		
toluene	92.14	0.87300		1	0.8730
monomer : initiator	1000				
porosity [%]:	80.34				

Procedure

The emulsion was prepared following the general procedure. The reaction mixture was transferred to a polypropylene mold and cured at 82°C for 33 minutes. Directly after removing the mold from the oven, the mixture was still liquid, yet highly viscous. It solidified upon cooling down to room temperature. The monolith was covered with a layer of acetone directly in the mold. To remove the surfactant, a small hole was cut into the mold at its bottom, the acetone was pumped through the monolith using pressurized air. After a while the “filtrate” turned yellow, indicating that the surfactant was washed out of the monolith. The sample was dried on air.

5.3.1.9. FPP84

Table 16 - reactants for reaction FPP84

	M [g/mol]	m [g]	n [mol]	V [mL]	ρ [g/mL]
cyclooctene	110.20	2.5500	2.31E-02	3	0.85
DCPD	132.20	0.1678	1.27E-03		0.98
Span 80	428.60	0.4137	9.65E-04		
H ₂ O		11			
M2	949.09	23.07	2.43E-05		
toluene	92.14	0.873		1	0.8730
monomer : initiator	1004 : 1				
porosity [%]:	75.390				

Procedure

The mixture was prepared according to the general procedure and cured for 30 min at 80°C. After being removed from the oven, the mixture was still viscous but solidified upon cooling to room temperature. A part of the brittle material was put into acetone and vacuum dried later on to prepare it for SEM measurements.

5. Experimental section

5.3.1.10. *FPP104*

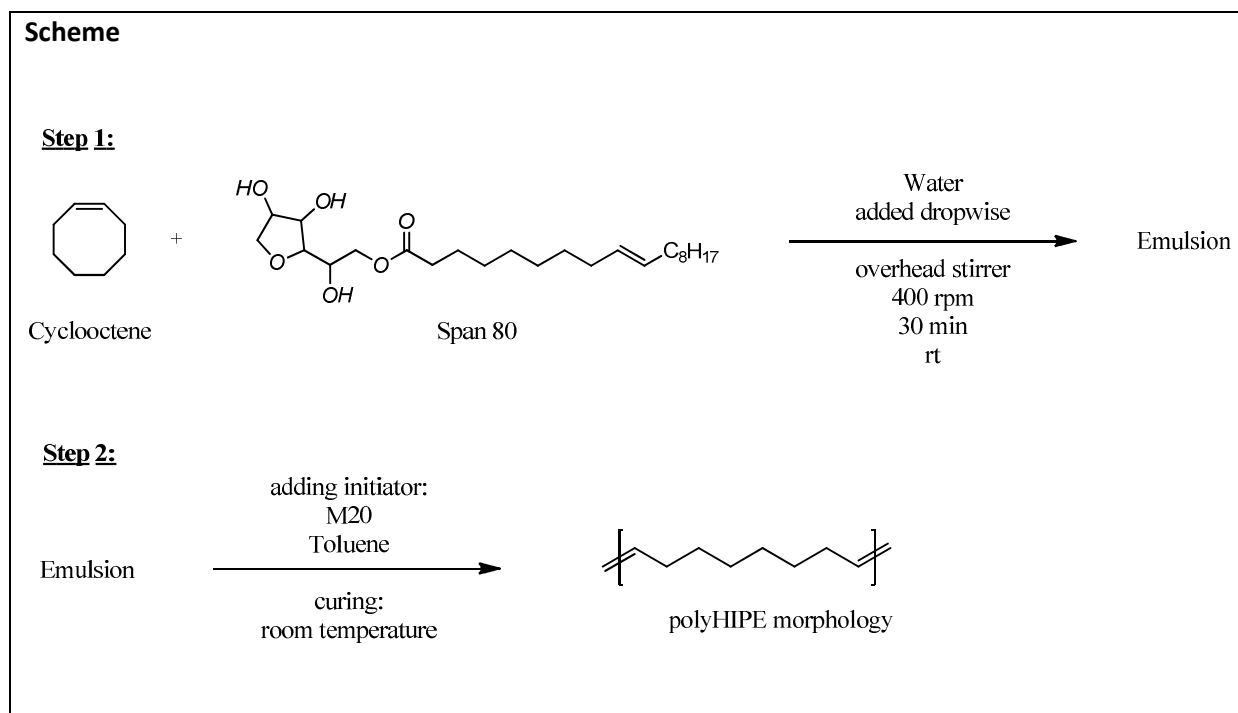


Table 17 - reactants for reaction FPP104

	M [g/mol]	m [g]	n [mol]	V [mL]	ρ [g/mL]
cyclooctene	110.20	2.21	2.01E-02	2.6	0.85
Span 80	428.60	0.3295	7.69E-04		
water		11			11
M20	929.95	9.16	9.85E-06		
toluene	92.14	0.5238		0.6	0.8730
monomer : initiator	2036 : 1				
porosity [%]:	80.1				

Procedure

The preparation was done like in reaction FPP55 using a different initiator (M20). The reaction mixture was transferred to a 20 mL glass vial, where the polymerization proceeded quickly. After 20 minutes a white, solid but very brittle monolith with plenty of fissures in the middle was obtained. Extraction with acetone in a soxhlet and vacuum drying were performed prior to SEM measurements.

Elemental Analysis

FPP 104	10.06.2011
%C	86.93
%H	12.64
%O	0.44

5. Experimental section

5.3.1.11. *FPP108*

Table 18 - reactants for reaction FPP108

	M [g/mol]	m [g]	n [mol]	V [mL]	ρ [g/mL]
cyclooctene	110.20	3.4	3.09E-02	4	0.85
Synperonic L121	4400.00	0.5108	1.16E-04		
H ₂ O		17			
M2	949.09	9.76	1.03E-05		
toluene	92.14	0.698		0.8	0.8730
monomer : initiator	3000				
porosity [%]:	80.6				

Elemental Analysis

FPP 108	25.05.2011	10.06.2011
%C	86.78	73.61
%H	12.57	10.42
%O	0.65	15.97

5.3.1.12. *FPP114*

Table 19 - reactants for reaction FPP114

	M [g/mol]	m [g]	n [mol]	V [mL]	ρ [g/mL]
DCPD	132.20	3.92	2.97E-02	4	0.98
Synperonic L121	4400.00	0.58	1.32E-04		
H ₂ O		19			
M2	949.09	4.69	4.94E-06		
toluene	92.14	0.873		0.8	0.8730
monomer : initiator	6001				
porosity [%]:	79.9				

Elemental Analysis

FPP 114	25.05.2011	10.06.2011
%C	73.35	62.07
%H	7.41	6.65
%O	19.23	31.27

5.3.2. Shouldered test bars

General procedure

The emulsion preparation follows the same procedure as for the preparation of porous monoliths. The amounts were calculated for a porosity of 80%. The reaction mixture with incorporated initiator solution was transferred to a preheated mold (80°C). After curing for 30 minutes, the mold was rapidly cooled down to room temperature in a cold water bath to avoid decomposition of the material. The solidified test bars were put in a glass bin and covered with acetone to extract the surfactant. This step was repeated several times before the test bars were dried in vacuo and measured at the tensile strength testing machine.

5.3.2.1. *polyCOE test bars*

	V [mL]	COE n [mol]	Synp. L121 m [g]	H₂O V [mL]	M2 m [mg]	M2 n [mol]	M2 : COE
FPP111	5.00	3.86E-02	0.6245	20.0	12.2	1.29E-05	1 : 3000
FPP113	7.00	5.40E-02	0.8724	29.0	17.1	1.80E-05	1 : 3000
FPP118	7.50	5.78E-02	0.9522	31.0	18.3	1.93E-05	1 : 3000
FPP120	7.50	5.78E-02	0.9516	31.0	18.4	1.94E-05	1 : 2982

5.3.2.2. *poly-COE-co-DCPD test bars*

	COE		DCPD		SL121	H₂O	M2		M2 : MM
	V [mL]	n [mol]	V [mL]	n [mol]	m [g]	V [mL]	m [mg]	n [mol]	
FPP121	7.50	5.78E-02	0.41	3.04E-03	1.0080	20.0	19.27	2.03E-05	1 : 2849
FPP122	7.50	5.78E-02	0.41	3.04E-03	1.0130	29.0	18.22	1.92E-05	1 : 3013
FPP123	7.50	5.78E-02	0.41	3.04E-03	1.0130	31.0	19.36	2.04E-05	1 : 2836

6. List of Figures

Fig. 1 - Schematic illustration of an emulsion	11
Fig. 2 - Sodium dodecyl sulfate - a typical anionic surfactant.....	12
Fig. 3 - steric stabilization of emulsion droplets	13
Fig. 4 - schematic illustration of the evolution of a freshly prepared emulsion	13
Fig. 5 – reaction mechanism of olefin metathesis	14
Fig. 6 – olefin metathesis reactions)	15
Fig. 7 - plot of ring strain and ring size from cyclic olefins for ROMP	15
Fig. 8 - reaction scheme for the preparation of biocompatible and -degradable porous monolithic materials from norbornene and functionalized oxanorbornene via ROMP.....	16
Fig. 9 - surface functionalization of polyHIPE material via living-polymerization	17
Fig. 10 – epoxidation of polyDCPD using MCPBA	17
Fig. 11 - location and type of allylic carbons in metathesis polymers	18
Fig. 12 - radical stability depending on substitution degree.....	18
Fig. 13 - SEM image of a typical polyHIPE morphology	20
Fig. 14 – schematic illustration of hypercrosslinking and functionalization of DVD-VBC-polyHIPE beads for the nucleophilic acylation of methylcyclohexanol.....	21
Fig. 15 - polyHIPE preparation via ROMP.....	22
Fig. 16 - COE-monolith after extraction with acetone.....	24
Fig. 17- Scheme for reaction FPP23	25
Fig. 18 - SEM images of FPP23-I.....	26
Fig. 19 - comparison of the morphologies of crosslinked cyclooctene (FPP23-I, 5 mol% DCPD; left) and not-crosslinked COE-monolith (FPP23-II; right)	27
Fig. 20 – comparison of FPP32a (left) and FPP32b (right)	28
Fig. 21 - emulsion stability test at 80°C.....	30
Fig. 22 - optical microscopy images of a W/O emulsion stabilized by Synperonic L121	30
Fig. 23 – M31 and M51; highly active initiators for polyHIPE preparation at low temperatures...	31
Fig. 24 - Evaporating dichloromethane generates large bubbles	33
Fig. 25 - SEM image from polyDCPD-monolith prepared with Span 80 (FPP30e)	35
Fig. 26 - morphology of pure polyCOE monolith (80% porosity).....	35
Fig. 27 - COE-co-DCPD-polyHIPE (5 mol% DCPD, 75% porosity; FPP 84)	36
Fig. 28 - M20: ROMP initiator bearing a PPh ₃ ligand	36
Fig. 29 - COE-polyHIPE prepared at room temperature exhibiting high open-cell morphology	37
Fig. 30 - FT-IR spectra of porous COE-monolith.....	39

7. List of Tables

Fig. 31 - FT-IR spectra of COE-polyHIPE	40
Fig. 32 - FT-IR spectra of DCPD-polyHIPE.....	42
Fig. 33 - DCPE-COE co-polyHIPEs with increasing COE concentration.....	44
Fig. 34 - Scanning electron microscopy images of co-polyHIPEs from DCPD and COE.....	44
Fig. 35 - “core-shell” structure of collapsed monoliths	45
Fig. 36 - shouldered test bars for tensile strength tests	46
Fig. 37 – tensile strength measurements of porous COE test bars	46
Fig. 38 – tensile strength measurements of porous COE-co-DCPD test bars	47
Fig. 39 – normalized refractive index chromatogram of different "L121" surfactants	49

7. List of Tables

Table 1 - COE-monolith preparation with increasing initiator loadings	24
Table 2 - emulsion compositions for stability test (FPP28).....	29
Table 3 – summary of monolith preparation using M31	31
Table 4 - overview for tested initiator loadings for Span 80 stabilized emulsions	33
Table 5 – amounts for the preparation of pure COE-, pure DCPD-, and co-polymer-monoliths ...	34
Table 6 - elemental analysis of porous polyCOE monoliths.....	40
Table 7 - elemental analysis of the COE polyHIPE	41
Table 8 - calculated elemental composition of polyCOE with copolymerized surfactant Span 80 .	41
Table 9 - elemental analysis of the DCPD polyHIPE.....	43
Table 10 – Young’s moduli (E), nominal strain (ϵ_M) and nominal stress (σ_M) of test bars	47
Table 11 - reactants for reaction FPP20/22	52
Table 12 - reactants for reaction FPP23-I	54
Table 13 - reactants for reaction FPP23-II	55
Table 14 - reactants for reaction FPP32.....	57
Table 15 - reactants for reaction FPP55.....	59
Table 16 - reactants for reaction FPP84.....	59
Table 17 - reactants for reaction FPP104.....	60
Table 18 - reactants for reaction FPP108.....	61
Table 19 - reactants for reaction FPP114.....	61

8. References

- ¹ Svec, F.; Fréchet, J. M. J. *Ind. Eng. Chem. Res.* **1999**, *38*, 34-48.
- ² Buchmeiser, M.R. *Polymer* **2007**, *48*, 2187-2198
- ³ Zhang, H.; Cooper, A.I. *Soft Matter* **2005**, *1*, 107-113
- ⁴ Svec, F. *J. Chromatogr. A* **2010**, *6*, 902-924.
- ⁵ Deleuze, H.; Faivre, R.; Herroque, V. *Chem. Commun.* **2002**, 2822-2823.
- ⁶ Evans, D.F.; Wennerström, H. *The colloidal domain* **1994**, 44.
- ⁷ Schramm, L.L. *Emulsions, Foams and Suspensions* **2005**, 76-81.
- ⁸ Paul, B.K.; Moulik, S.P. *Current Science* **2001** *80*, 990-1001.
- ⁹ Schramm, L.L. *Emulsions, Foams and Suspensions* **2005**, 97-100.
- ¹⁰ Butt, H.J.; Graf, K.; Kappl, M. *Physics and chemistry of interfaces* **2003**, 259.
- ¹¹ Cameron, N.R. *Polymer* **2005**, *46*, 1439-1449.
- ¹² Evans, D.F.; Wennerström, H. *The colloidal domain* **1994**, 485-490.
- ¹³ De Smet, Y.; Deriemaeker, L.; Finsy, R. *Langmuir* **1999**, *15*, 6745-6754.
- ¹⁴ Bancroft, W.D. *J. Phys. Chem.* **1912**, *16*, 177-233.
- ¹⁵ ICI Americas Inc.: Wilmington, *The HLB System*, **1976**.
- ¹⁶ Trnka, T.M.; Grubbs, R.H. *Acc. Chem. Res.* **2001**, *34*, 18-29.
- ¹⁷ Hérisson, J.-L.; Chauvin, Y. *Makromol. Chem.* **1971**, *141*, 161-167.
- ¹⁸ Leitgeb, A.; Wappel, J.; Slugovc, C. *Polymer* **2010**, *51*, 2927-2946.
- ¹⁹ Lerum, M.F.Z.; Chen, W. *Langmuir* **2011**, *27*, 5403-5409.
- ²⁰ Löber, A.; Verch, A.; Schlemmer, B.; Höfer, S.; Frerich, B.; Buchmeiser, M.R. *Angew. Chem.* **2008**, *120*, 9278-9281.
- ²¹ Bielawski, C.W.; Grubbs, R.H. *Prog. Polym. Sci.* **2007**, *32*, 1-29.
- ²² Wolfberger, A.; Rupp, B.; Kern, W.; Griesser, T.; Slugovc, C. *Macromol. Rapid Commun.* **2011**, *32*, 518-522.
- ²³ Perring, M.; Long, T.R.; Bowden, N.B. *J. Mater. Chem.*, **2010**, *20*, 8679-8685.
- ²⁴ Clayden J., Greeves N., Warren S., Wothers P. *Organic Chemistry* **2001**, 1026-1027.
- ²⁵ D. Barby and Z. Haq, *Eur. Pat.* **1982**, *60*, 138.
- ²⁶ Kimmins, S.D.; Cameron, N.R. *Adv. Funct. Mater.* **2011**, *21*, 211-225.
- ²⁷ Pierre, S. J.; Thies, J. C.; Dureault, A.; Cameron, N. R.; van Hest, J. C. M.; Carette, N.; Michon, T.; Weberskirch, R. *Adv. Mater.* **2006**, *18*, 1822-1826.
- ²⁸ Brown, J.F.; Krajnc, P.; Cameron, N.R. *Ind. Eng. Chem. Res.* **2005**, *44*, 8565-8572.
- ²⁹ Hainey, P.; Huxham, I.M.; Rowatt, B.; Sherrington, D.C. *Macromolecules* **1991**, *24*, 117-121.

- ³⁰ Pulko, I.; Wall, J., Krajnc, P.; Cameron, N.R. *Chem. Eur. J.* 2010, **16**, 2350 – 2354.
- ³¹ Kovačič, S.; Štefanec, D.; Krajnc, P. *Macromolecules* **2007**, **40**, 8056-8060.
- ³² Gokmen, M.T; Van Camp, W.; Colver, P.J.; Bon, S.A.F.; Du Prez, F.E. *Macromolecules* **2009**, **42**, 9289–9294.
- ³³ Benmachou, K.; Deleuze, H.; Heroguez, V. *Reactive & Functional Polymers* **2003**, **55**, 211–217.
- ³⁴ Kovačič, S.; Krajnc, P.; Slugovc C. *Chem. Commun.*, **2010**, **46**, 7504–7506
- ³⁵ Vestenamer® product information sheet:
http://www.degussa-hpp.de/dl/pi2/VMER%208012_e9_ad.pdf, 26-05-2011.
- ³⁶ Barbetta, A.; Cameron, N. R. *Macromolecules* **2004**, **37**, 3188-3201
- ³⁷ Lumelsky, Y.; Silverstein, M. S. *Macromolecules* **2009**, **42**, 1627-1633
- ³⁸ Broggi, J.; Urbina-Blanco, C. A.; Clavier, H.; Leitgeb, A.; Slugovc, C.; Slawin; A. M. Z.; Nolan, S. P. *Chem. Eur. J.* **2010**, **16**, 9215 – 9225
- ³⁹ Schlemmer, B.; Gatschelhofer, C.; Pieber, T.R.; Sinner, F.M.; Buchmeiser, M.R. *J. Chromatogr. A* **2006** **1132**, 124-131
- ⁴⁰ Socrates, G. *Infrared Characteristic Group frequencies*, **1994**, 2nd edition.
- ⁴¹ Long, T.R.; Gupta, A.; Lee Miller II, A.; Rethwisch, D.G.; Bowden, N.B. *J. Mater. Chem.* **2011**, early publication.
- ⁴² Kovačič, S.; Slugovc C. **2011**, unpublished results
- ⁴³ Mühlebach, A.; van der Schaaf, P.A.; Hafner, A.; Setiabudi, F. *J. Mol. Catal. A: Chem.* **1998**, **132**, 181–188.